Green Optical Communications—Part I: Energy Limitations in Transport

Rodney S. Tucker, *Fellow, IEEE*

(Invited Paper)

***Abstract*—The capacity and geographical coverage of the global communications network continue to expand. One consequence of this expansion is a steady growth in the overall energy consumption of the network. This is the first of two papers that explore the fundamental limits on energy consumption in optical communication systems and networks. The objective of these papers is to provide a framework for understanding how this growth in energy consumption can be managed. This paper (Part I) focuses on the energy consumption in optically amplified transport systems. The accompanying paper (Part II) focuses on energy consumption in networks. A key focus of both papers is an analysis of the lower bound on energy consumption. This lower bound gives an indication of the best possible energy efficiency that could ever be achieved. The lower bound on energy in transport systems is limited by the energy consumption in optical amplifiers, and in optical transmitters and receivers. The performance of an optical transport system is ultimately set by the Shannon bound on receiver sensitivity, and depends on factors such as the modulation format, fiber losses, system length, and the spontaneous noise in optical amplifiers. Collectively, these set a lower bound on the number of amplifiers required, and hence, the amplifier energy consumption. It is possible to minimize the total energy consumption of an optically amplified system by locating repeaters strategically. The lower bound on energy consumption in optical transmitters and receivers is limited by device and circuit factors. In commercial optical transport systems, the energy consumption is at least two orders of magnitude larger than the ideal lower bounds described here. The difference between the ideal lower bounds and the actual energy consumption in commercial systems is due to inefficiencies and energy overheads. A key strategy in reducing the energy consumption of optical transport systems will be to reduce these inefficiencies and overheads.**

***Index Terms*—Energy consumption, energy efficiency, optical amplifiers, optical fiber transport, optical receivers, optical transmitters.**

I. Introduction

COMMUNICATIONS technologies have produced enormous societal change during the 160-year period, since the first telegraph systems were installed in the 1840s. Over this period, communications technology has moved from being a luxury that few could afford, to an indispensible element of everyday life for many people. This transformation has been brought about by two key factors: an enormous increase in system capacity and a dramatic reduction in the real cost of communications technologies. The transmission capacity of communication links has increased from a few bits per second, in the early days of telegraph systems, to many terabits per second today—an increase in data rate of more than 12 orders of magnitude. Sustained improvements in electronic technologies, and especially in recent years, advances in silicon IC technologies and optoelectronic device technologies, together with the economies of mass production, have brought cutting-edge technology within the reach of everyone.

Many papers in the literature, and indeed in the pages of this journal, have described technological advances that have led to lower cost and higher capacity communications. This paper and the accompanying paper [1] discusses a third key consideration: energy consumption in optical systems and networks. "Green" communications is not a new topic—energy consumption has always been an important consideration in communications system design. In fact, it is arguable that much of the improvement in communications system capacity over the past 160 years would not have been possible without dramatic improvements in energy efficiency of transmission technology. However, today, in the early 21st century, the issue of energy consumption in information technology and communications systems takes on increased importance [2] due to the growing realization that we live in an energy-constrained world. As shown in [3] and [4], the global Internet consumes a small, but growing proportion of the planet's electricity supply.

The objective of this paper is to explore the fundamental limits on energy consumption in optical transport systems. The basis of the analysis is a simple, but powerful metric: the energy consumption per bit of data transported. We show in this paper how this metric can assist in developing and comparing strategies for the design of more energy-efficient transport systems. In the accompanying paper (Part II) [1], we show how this metric for energy consumption enables a broad picture, to be established, of the energy consumption in optical communications networks.

This paper examines the lower bound on energy consumption in optically amplified fiber transmission systems. This lower bound on energy is limited by energy consumption in optical amplifiers and in the optical transmitters and receivers. The performance of an optical transport system is ultimately set by the Shannon bound on receiver sensitivity, and depends on factors, such as the modulation format, fiber losses, system length, and the spontaneous noise inherent in optical amplifiers. Collectively, these set a lower bound on the

Manuscript received February 26, 2010; revised May 11, 2010; accepted May 18, 2010. Date of publication August 2, 2010; date of current version April 6, 2011. This work was supported in part by the Australian Research Council and in part by Cisco Systems.

The author is with the Department of Electrical and Electronic Engineering, University of Melbourne, Parkville, Vic. 3010, Australia (e-mail: r.tucker@unimelb.edu.au).

Color versions of one or more of the figures in this paper are available online at http://ieeexplore.ieee.org.

Digital Object Identifier 10.1109/JSTQE.2010.2051216

number of amplifiers required, and hence, the amplifier energy consumption.

In determining the lower bound on energy consumption in transport systems, it is necessary to consider the energy of the optical transmitters and receivers used in the end terminals and in intermediate repeaters. We show that it is possible to minimize the total energy consumption of an optically amplified system that incorporates appropriately located repeaters by optimizing the spacing between the repeaters.

It is also necessary to consider the influence of the modulation format on the energy consumption. Advanced modulation formats with high-spectral efficiency are an effective way to maximize the capacity of a single fiber. However, at the ideal lower bound of energy consumption, advance modulation formats, such as quadratic-amplitude modulation (QAM) are less energy efficient than simple modulation formats, such as on–off keying (OOK).

There is no easily defined absolute lower bound on the energy consumption of optical transmitters and receivers. However, our analysis provides an indication of the minimum achievable energy consumption in typical optical transmitter and receiver circuits. We show that the difference between the ideal lower bounds described in this paper and the actual energy consumption in commercial systems can be accounted for in terms of device and circuit inefficiencies, and energy overheads. We argue that a key strategy in reducing the energy consumption of optical transport systems will be to reduce these inefficiencies and overheads.

The paper is organized as follows. Section II provides an historical perspective on the energy consumption of communications systems. Section III analyzes the lower bound on energy consumption in optical transport, with a focus on optically amplified transmission systems. Section IV covers the lower bound on energy consumption of optical transmitters and receivers and in Section V we examine how the differences between the ideal lower bounds obtained in Sections III and IV and real-world devices are due to energy inefficiencies and overheads. In Section IV, we consider the influence of modulation format on energy consumption. In Part II [1], we extend the analysis to include the lower bounds on energy consumption in optical networks.

II. Historical Perspective

The energy efficiency of long-haul wireline systems has improved greatly over time. Fig. 1 shows the historical evolution of energy per bit in transoceanic communications systems. For convenience, the energy per bit in Fig. 1 is normalized to a transmission distance of 1000 km. Note that some transoceanic systems operate over longer distances than this. The first trans-Atlantic telegraph system became operational late in the 1850s. It had no repeaters, and its transmission capacity was limited by the capacitance of the transmission line. The energy per bit in this system was essentially the energy expended in charging and discharging this capacitance.

The early trans-Atlantic wireless systems were initially very energy hungry, but by the 1930s, the energy per bit in telegraph and wireless systems were similar, at around 0.1 J/b/1000 km. The early undersea coaxial systems (e.g., TAT1–TAT5) saw further reductions in energy per bit, and this trend continued with first-generation optical systems, using optoelectronic repeaters.

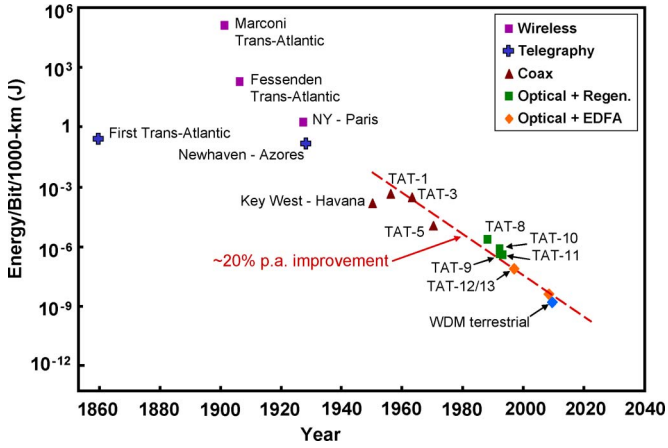

Fig. 1. Energy per bit per 1000 km of transmission distance for various transatlantic transmission systems.

TABLE I
Representative Energy Consumption Per Bit in 2010-Era 1000-km Commercial Transport System (40 × 40 Gb/s)

		TX/RX	Amplifier	Total
Power consumption per Device (40 wavelengths)		800 W	100 W	
Energy per Bit per Device		500 pJ	60 pJ	
1,000-km System	Number of Devices	1	10	
	Energy per Bit	500 pJ	600 pJ	1.1 nJ

Second-generation optical systems using optical amplifiers have enabled the energy per bit to be reduced to approximately 10 nJ/b/1000-km. Over the period 1960 to 2010, Fig. 1 shows that the energy efficiency of transoceanic systems has been falling exponentially, with a rate of improvement of around 20% per annum, as shown by the trend line (broken line). For comparison, Han [5] presents the power consumption and capacity of terrestrial optical transport platforms over the period 1990–2008, which suggests that the energy efficiency of these systems has been improving at a rate of about 15% per annum.

Fig. 1 includes a data point for a representative 1000-km unrepeatered terrestrial system using 2010 generation technology based on typical data from a number of equipment manufacturers, e.g., [6] and [7]. To determine the energy per bit in this system, the total power consumption of each item of equipment is divided by the number of wavelengths (40) and by the bit rate (40 Gb/s). The total energy consumption of this system is 1.1 nJ/b. Table I gives a break down of the contributions to this energy, showing that the energy consumption is in the optical amplifiers is about the same as in the transmitter/receiver pair. For systems with reach other than 1000 km, the balance between amplifiers and the transmitter/receiver pair would be different.

III. Energy Consumption in Optical Transport

A. System Energy Model

Continuous improvements in lightwave transmission technology have led to ever-increasing transmission capacities in optical fiber. Some of the key technology challenges and fundamental

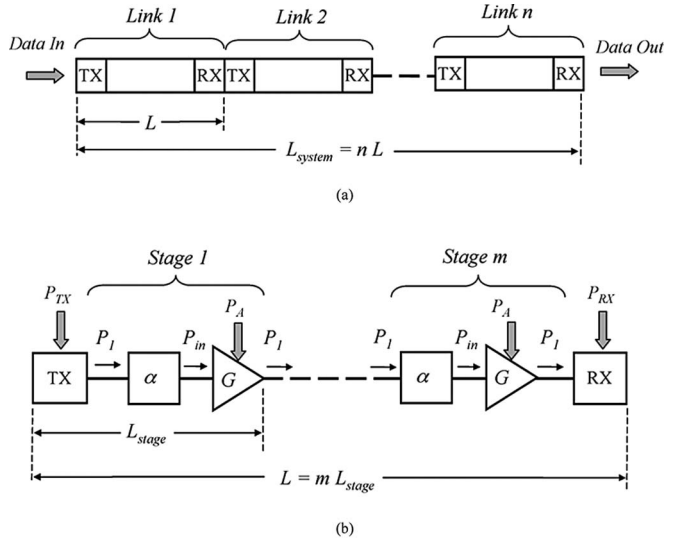

Fig. 2. WDM transmission system of length $L_{\rm system}$. (a) Overall schematic of system, comprising n identical optically amplified links, each of length L. (b) Schematic of optically amplified link, comprising an optical transmitter, m identical stages of optical gain, and an optical receiver. Each stage has length $L_{\rm stage}$.

limitations on fiber capacity are summarized in [8] and [9]. In this section, we focus on another limitation on fiber transmission system capacity—the energy consumption. To quantify the energy consumption we use the energy per bit of data, or simply the energy per bit. This is a fundamental measure of energy efficiency in digital communications systems [3]. It is sometimes expressed in units of power per bit rate (e.g., W/b/s or W/Gb/s [10]).

The objective of Section III is to present a picture of the key contributors to energy consumption in optical transport and to identify the lower limits. It is well known that optical transport accounts for only a small part of the total energy consumption of the Internet [3], [4]. However, as the capacity of the network increases, there is a growing need to understand how to manage energy consumption in transport as part of a holistic approach to managing energy consumption in the network. The analysis in this section provides a framework for understanding the theoretical bounds on the energy consumption of optical transport.

Our analysis is based on the model shown in Fig. 2(a) of a multilink wavelength-division multiplexing (WDM) transmission system. The transmission system comprises n identical optically amplified links. Each link has length L and the overall length of the system is nL. A WDM transmitter/receiver (TX/RX) pair at the interface between each link provides regenerated signals at each wavelength for injection in the next link of the system. Fig. 2(b) shows a schematic of one of the n identical optical-amplified links of system in Fig. 2(a). The link is terminated with a WDM optical transmitter at the input and a WDM optical receiver at the output. The transmitter, receiver, and amplifiers support k wavelengths. Each link [see Fig. 2(b)] comprises m identical stages, each of length (i.e., amplifier spacing) $L_{\rm stage}$. The total length of each link is $L = mL_{\rm stage}$.

Each stage in Fig. 2(b) is modeled by a fiber attenuation block with a power loss of $D = e^{\alpha L_{\rm stage}}$, where α is the power attenuation per unit length of the fiber, and an amplifier gain block with power gain G, which is equal to the loss per stage (i.e., $G = D$). There are $(m-1)$ line amplifiers and one amplifier preceding the receiver, giving a total of m amplifiers. The link has an optical bandwidth B_o. Each amplifier contains optical filters [not shown in Fig. 2(b)] that match the optical bandwidth of the link to the optical spectrum of the optical transmitter. For simplicity, we assume that the optical gain G is the same at all signal wavelengths and that the optical signal power is the same at all wavelengths. Note that the analysis here focuses on fundamental limitations on energy consumption. For this reason, the model in Fig. 2 does not include system impairments due to dispersion and other nonideal behavior of the transport medium. Different fiber types introduce different levels of dispersion. This dispersion requires compensation and possibly introduces a need for additional amplification. Although important, this falls outside the province of this calculation of the lower bound.

The total power $P_{\rm tot}$ consumed by the transmission link in Fig. 2(b) is given by

$$P_{\rm tot} = mP_A + P_{\rm TX/RX} \tag{1}$$

where P_A is the supply power to each amplifier, $P_{\rm TX/RX} = P_{\rm TX} + P_{\rm RX}$ is the supply power to each WDM transmitter/receiver pair, and $P_{\rm TX}$ and $P_{\rm RX}$ are the transmitter and receiver supply powers, as shown in Fig. 2. At each wavelength, the signal input power and output power at the input and output of each amplifier are $P_{\rm in}$ and P_1, respectively, as shown in Fig. 2(b). The signal input power at each wavelength can be written as $P_{\rm in} = P_1 e^{-\alpha L_{\rm stage}}$ The well-known power conversion equation for the k WDM channels can be written as $k(P_1 - P_{\rm in}) = \eta_{\rm PCE} P_P$, where $\eta_{\rm PCE}$ is the amplifier power conversion efficiency and P_P is the amplifier pump power [11].

The maximum achievable power conversion efficiency is $\eta_{\rm PCE} = \lambda_p/\lambda_s$, where λ_p is the pump wavelength and λ_s is the signal wavelength [11]. The pump power P_P is related to the total amplifier supply power P_A via the expression $P_P = \eta_E P_A$, where η_E is the power conversion efficiency of the amplifier control and management circuitry, including the temperature controllers and the pump laser. Combining these equations, we obtain $P_1 = P_{\rm in} + \eta_{\rm EPCE} P_A/k$, where $\eta_{\rm EPCE} = \eta_E \eta_{\rm PCE}$ is the overall electrical power conversion efficiency of the amplifier [11].

B. Lower Bound on Energy Consumption of Optically Amplified Transport

We now focus on determining the lower limit or lower bound on transport energy using the power consumption model of the optically amplified transmission link presented in Section III-A earlier. We will show later how this lower bound on energy consumption provides a useful benchmark for comparing energy in different transmission systems.

At each wavelength, the optical SNR (OSNR) of the output of stage m in each optically amplified link is given by [11]

$$\text{OSNR} = \frac{P_1}{2n_{\rm sp}\, m(e^{\alpha L_{\rm stage}} - 1) h\nu\, B_o} \tag{2}$$

where P_1 is the average signal power at the output of the transmitter and each of the amplifiers, $n_{\rm sp}$ is the spontaneous emission factor of each of the amplifiers, h is Plank's constant, and ν is the optical frequency.

It is convenient to express (2) in terms of the SNR per bit, which is the ratio of signal energy to noise energy integrated over one bit period. The SNR per bit $\mathrm{SNR}_{\rm bit}$ is given by $\mathrm{SNR}_{\rm bit} = 2\tau_{\rm bit} B_o \,\mathrm{OSNR}$, where $\tau_{\rm bit}$ is the bit period [12]. Thus, the energy per bit of the optical signal at the output of the mth amplifier is given by

$$E_1 = P_1 \tau_{\rm bit} = \mathrm{SNR}_{\rm bit}\, n_{\rm sp} m (e^{\alpha L_{\rm stage}} - 1) h\nu. \quad (3)$$

Combining (1) and (3), the total energy per bit per wavelength consumed by all active devices in the optically amplified link is $E_{\rm bit} = P_{\rm tot}\tau_{\rm bit}/k$ as follows:

$$E_{\rm bit} = E_{\rm AMP} + E_{\rm TX/RX} \quad (4)$$

where

$$E_{\rm AMP} = \frac{mP_A\tau_{\rm bit}}{k} = \frac{\mathrm{SNR}_{\rm bit}\, n_{\rm sp} m^2 (e^{\alpha L_{\rm stage}} - 1)(1 - e^{-\alpha L_{\rm stage}}) h\nu}{\eta_{\rm EPCE}} \quad (5)$$

is the total energy per bit per wavelength in the amplifiers and $E_{\rm TX/RX} = P_{\rm TX/RX}\tau_{\rm bit}/k$ is the energy per bit per wavelength in the transmitter/receiver pair. In Section IV, we carry out a detailed analysis of the $E_{\rm TX/RX}$ term in (4). But before considering the $E_{\rm TX/RX}$ term, we will explore the lower limits on the $E_{\rm AMP}$ term in (4).

In order to determine the theoretical lower limit on the amplifier energy per bit $E_{\rm AMP}$, we set the power conversion efficiency $\eta_{\rm PCE}$ to its theoretical maximum value of $\sim$1.0 for an erbium-doped fiber amplifier (EDFA) with a pump wavelength near 1480 nm, and signal wavelengths around 1550 nm. In addition, we set $\eta_E = 1.0$, the spontaneous emission factors $n_{\rm sp}$ of the amplifiers to unity, and assume zero coupling loss at the input and output of the amplifier. Note that these parameters are for an ideal amplifier and practical EDFA's fall short of this by a few decibel (dB). Thus, for ideal amplifiers (5) reduces to

$$E_{\text{AMP-min}} \simeq \mathrm{SNR}_{\rm bit}\, m^2 (e^{\alpha L_{\rm stage}} - 1)(1 - e^{-\alpha L_{\rm stage}}) h\nu \quad (6)$$

where $E_{\text{AMP-min}}$ is the theoretical lower limit on $E_{\rm AMP}$.

Fig. 3 is a plot of $E_{\text{AMP-min}}$ as a function of the amplifier spacing $L_{\rm stage}$ for a total transmission distance $L = 2000$ km and with a fiber loss of 0.2 dB/km, and a wavelength of 1.55 μm. The data are presented for OOK and differential binary phase-shift keying (DBPSK) with a bit error rate (BER) of 10^{-9}. For this error rate, the required SNR per bit is 16.1 dB for OOK and 13.4 dB for DBPSK [12]. Not surprisingly, the well-known $\sim$3-dB system sensitivity advantage of DBPSK over OOK [12], as indicated by these $\mathrm{SNR}_{\rm bit}$ values, translates into DBPSK achieving a lower bound on total system energy per bit. An even more energy-efficient modulation format is eight-level dual-polarization quaternary phase-shift keying (DP-QPSK) [13]. This modulation format gives a 1-dB improvement over DBPSK.

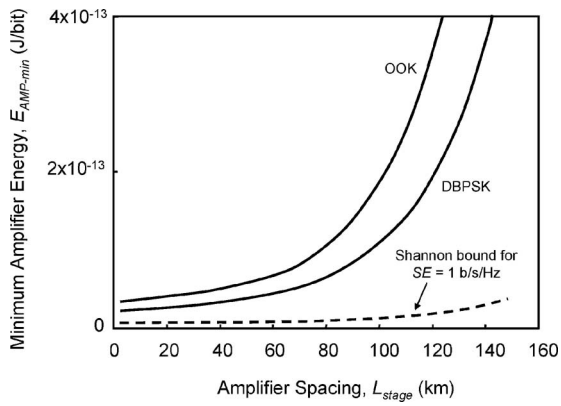

Fig. 3. Minimum total amplifier energy per bit for 2000-km optically-amplified system as a function of amplifier spacing. The fiber loss is 0.2 dB/km and the SNR per bit is 16.1 dB for OOK and 13.4 dB for DBPSK.

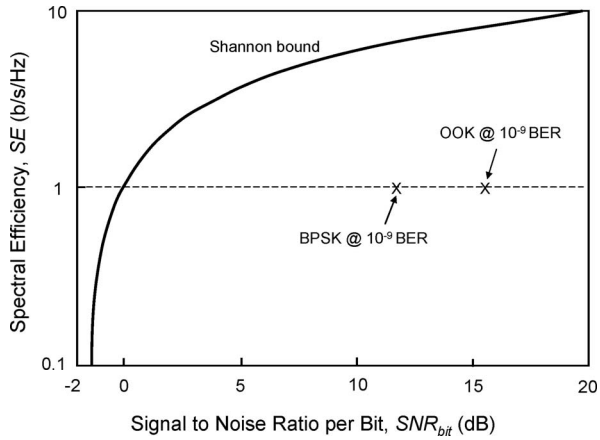

Fig. 4. Spectral efficiency versus $\mathrm{SNR}_{\rm bit}$, showing Shannon bound.

Fig. 4 shows the spectral efficiency (SE) in bits per second per hertz as a function of $\mathrm{SNR}_{\rm bit}$. The solid line is the well-known Shannon bound [14], given by

$$\mathrm{SE} = \log_2(1 + \mathrm{SE}\cdot \mathrm{SNR}_{\rm bit}). \quad (7)$$

Note that (7) is in a form that some readers may not be familiar with. For a derivation of (7), the reader is referred to [14] or [9]. Equation (7) assumes sinc function signaling pulses and zero guard bands [9].

Also shown in Fig. 4 are the locations of points representing the OOK and BPSK data shown in Fig. 3. The horizontal broken line in Fig. 4 represents a spectral efficiency of 1 b/s/Hz. At this spectral efficiency, the Shannon bound is $\mathrm{SNR}_{\rm bit} = 0$ dB. Fig. 3 shows $E_{\text{AMP-min}}$ (broken line) at the Shannon bound for this spectral efficiency.

In principle, the receiver sensitivity can be improved by forward error correction (FEC) using methods, such as turbocoding or low-density parity-check coding [15]. Coding gains in excess of 10 dB and receiver performances very close to the Shannon bound have been demonstrated using a variety of coding techniques [15], [16]. While FEC can improve receiver sensitivity, and therefore, improve the energy efficiency of transport, FEC itself consumes energy [17], and this energy cost needs to be

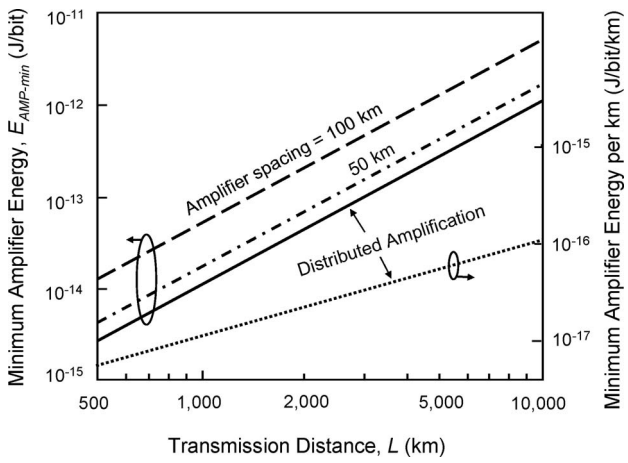

Fig. 5. Minimum amplifier energy per bit for optically amplified system with OOK and amplifier spacing of 50 and 100 km, and with distributed amplification. Also shown is the minimum amplifier energy per bit per kilometer of transmission distance for distributed amplification. The energy per bit per kilometer for lumped amplifiers has the same slope as this curve, but the absolute values increase with amplifier spacing. The fiber attenuation is 0.2 dB/km.

traded off against the reduction in transport energy efficiency that results from its use.

To obtain a feel for the energy tradeoff involved in coding, consider the 2000-km system in Fig. 3, with an amplifier spacing of 100 km. In this system, the minimum amplifier energy per bit for BPSK without decoding is about 100 fJ larger than the minimum amplifier energy for operation at the Shannon bound. Therefore, if the energy per bit required for coding and decoding is more than 100 fJ, there would be no energy advantage in using this coding and decoding. In Part II [1], we show that the energy consumption per transistor logic level transition in a 2009-era 45-nm CMOS IC (including intrachip interconnects) is about 3 fJ. Therefore, coding and decoding would need to use fewer than 35 transistor logic level transitions per bit, if an energy benefit is to be obtained. FEC is computationally intensive [17], and requires considerably more than 70 logic level transitions per bit. Current commercial FEC chips (see, for example, [18]), operating at 40 Gb/s consume around 250 pJ/b. However, future generations of CMOS technology may eventually provide energy-efficient FEC in the context of this analysis. Note that FEC is effective in reducing the impact of degradations in system performance due to dispersion and other system impairments. A comparison of the energy efficiency of FEC compared with the energy efficiency of other methods for reducing the impact of impairments is beyond the scope of this paper.

Fig. 5 shows $E_{\mathrm{AMP\text{-}min}}$ as a function of the total transmission distance, for OOK systems with amplifier spacing of 50 and 100 km. As before, the SNR per bit at the receiver is 16.1 dB. For a 1000-km link, the transport energy $E_{\mathrm{AMP\text{-}min}}$ with a 100-km amplifier spacing is about 0.2 pJ/b, and for a 10 000-km system, it is 5 pJ/b.

So far, we have considered amplified links using lumped amplifiers. However, the smallest energy per bit is achieved with zero amplifier spacing (i.e., with distributed amplification) [19]. Putting $L_{\mathrm{stage}} = L/m \to 0$ in (5), we obtain the minimum amplifier energy $E_{\mathrm{AMP\text{-}dist}}$ for a system with distributed amplification

$$E_{\mathrm{AMP\text{-}dist}} = \mathrm{SNR}_{\mathrm{bit}} (\alpha L)^2 h \nu. \tag{8}$$

From (8), $E_{\mathrm{AMP\text{-}dist}}$ for the 2000-km link in Fig. 3 is 44 fJ/b for OOK and 24 fJ/b for DBPSK, and 4.4 fJ/b at the Shannon bound for a spectral efficiency of SE = 1 b/s/Hz.

Fig. 5 shows the minimum amplifier energy per bit $E_{\mathrm{AMP\text{-}dist}}$ for a system using distributed amplification and also the minimum amplifier per bit per kilometer of transmission distance for distributed amplification. Note that the amplifier energy per bit decreases as the amplifier spacing is decreased and reaches a minimum for distributed amplification. This can also be seen in Fig. 3, where the curves for $E_{\mathrm{AMP\text{-}min}}$ asymptote to $E_{\mathrm{AMP\text{-}dist}}$ as the amplifier spacing approaches zero. The reason why the energy is minimum for distributed amplification is that amplified spontaneous emission (ASE) noise builds up less rapidly with distance in systems with shorter repeater spans. The minimum rate of build up of noise occurs with distributed amplification.

Commercial amplifiers consume much more energy than the lower bound. The intrinsic power conversion efficiency η_{PCE} for 980-nm pumps is $\sim$63%, and for 1480-nm pumps, it is $\sim$95%. Including coupling and other losses, the actual η_{PCE} of commercial devices is typically in the range of 40% and the electrical power conversion efficiency η_{EPCE} of commercial amplifiers is typically around 1% [11]. Therefore, practical systems using today's technology typically consume at least two orders of magnitude more power than the lower bound.

C. Optimum Repeater Spacing

Equation (5) shows that for a fixed stage length L_{stage}, the amplifier energy in an optically amplified system increases as square of the number of stages m of amplification. This square law increase in energy consumption is associated with a build up of ASE as the number of stages increases. Optoelectronic transmitter/receiver pairs (i.e., repeaters) placed strategically along the transmission path can control this build up of ASE, and thereby, control the square law increase in energy consumption. In this context, a key question is: for a fixed overall system length L_{system} and for a given amplifier spacing L_{stage} (usually determined in advance by the location of equipment huts in the field), what is the optimum spacing of optoelectronic repeaters in these equipment huts to minimize the lower bound on energy consumption in the optically amplified system in Fig. 2(a)? In other words, what is the optimum number of links n in Fig. 2(a) or equivalently, the optimum number of amplifiers per stage in Fig. 2(b)? A second key question is: what is the minimum energy consumption per bit per unit transmission distance when n is optimized?

To answer these questions, we need to consider the end-to-end energy per bit (per wavelength) $E_{\mathrm{bit,system}}$ in the transport system in Fig. 2(a). This energy is converted to energy per bit per unit transmission distance by dividing by the total transmission distance L_{system}. Because $E_{\mathrm{bit,system}} = nE_{\mathrm{bit}}$ and $L_{\mathrm{system}} = nL$, it follows that the total system energy per bit per unit transmission distance can be written as

$E_{\mathrm{bit,system}}/L_{\mathrm{system}} = E_{\mathrm{bit}}/L$, and the problem can be solved by focusing on the quantity E_{bit}/L. For fixed amplifier spacing $L_{\mathrm{stage}} = L/m$, the total system energy per bit per unit transmission distance is as follows:

$$\frac{E_{\mathrm{bit}}}{L} = \frac{E_{\mathrm{AMP}}}{mL_{\mathrm{stage}}} + \frac{E_{\mathrm{TX/RX}}}{mL_{\mathrm{stage}}}. \tag{9}$$

Note that all energies in (9) are energies per bit per wavelength. By substituting (5) in (9), differentiating with respect to m, and setting the derivative to zero, it is easy to show that the optimum repeater spacing L_{opt} for minimum overall energy consumption per bit is achieved when

$$E_{\mathrm{AMP}} = E_{\mathrm{TX/RX}} \tag{10}$$

i.e.,

$$m_{\mathrm{opt}} P_A = P_{\mathrm{TX/RX}} \tag{11}$$

where m_{opt} is the optimum value of m. Equation (11) shows that the overall energy consumption per bit per unit transmission distance is optimized (i.e., minimum), when the repeater spacing is selected so that the total energy (or power) consumed by all of the amplifiers in each link is the same as the energy (or power) consumed by the transmitter and receiver for this link. If the repeater spacing is larger than this optimum value, the total energy consumed by the amplifiers exceeds the total energy in the transmitter and receiver. Conversely, if the repeater spacing is less than the optimum value, the total energy consumed by the amplifiers is less than the total energy in the transmitter and receiver.

The optimum value of m for minimum overall energy consumption per bit per unit transmission distance is given by

$$m_{\mathrm{opt}} = \sqrt{\frac{E_{\mathrm{TX/RX}}\eta_{\mathrm{EPCE}}}{\mathrm{SNR}_{\mathrm{bit}}\, n_{\mathrm{sp}}(e^{\alpha L_{\mathrm{stage}}} - 1)(1 - e^{-\alpha L_{\mathrm{stage}}})h\nu}}. \tag{12}$$

Substituting (12) and (5) in (9), we obtain $(E_{\mathrm{bit}}/L)_{\mathrm{opt},L}$ the optimum (i.e., minimum) energy per bit per wavelength per unit transmission distance for a system with lumped amplification and when the repeater spacing is optimized to minimize E_{bit}/L

$$\left(\frac{E_{\mathrm{bit}}}{L}\right)_{\mathrm{opt},L} = \frac{2\sqrt{\mathrm{SNR}_{\mathrm{bit}}\, n_{\mathrm{sp}}(e^{\alpha L_{\mathrm{stage}}} - 1)(1 - e^{-\alpha L_{\mathrm{stage}}})h\nu E_{\mathrm{TX/RX}}}}{L_{\mathrm{stage}}\sqrt{\eta_{\mathrm{EPCE}}}}. \tag{13}$$

For distributed amplification, the optimum energy per bit per wavelength per unit transmission distance is $(E_{\mathrm{bit}}/L)_{\mathrm{opt},D}$, and for distributed amplification (13) becomes

$$\left(\frac{E_{\mathrm{bit}}}{L}\right)_{\mathrm{opt},D} = 2\alpha\sqrt{\frac{\mathrm{SNR}_{\mathrm{bit}}\, n_{\mathrm{sp}} h\nu E_{\mathrm{TX/RX}}}{\eta_{\mathrm{EPCE}}}}. \tag{14}$$

Fig. 6(a) shows the optimum repeater spacing $m_{\mathrm{opt}}L_{\mathrm{stage}}$, obtained from (12), and the energy per bit per kilometer, obtained from (13), against amplifier spacing L_{stage} for two representative scenarios. The broken curves apply to typical state-of-the-art 2010-era technologies, with an amplifier electrical power conversion efficiency η_{EPCE} of 1% and a transmitter/receiver energy per bit $E_{\mathrm{TX/RX}}$ of 30 pJ/b (see Section IV for a detailed analysis of transmitter and receiver energy consumption). The solid curves apply to an ideal future system with $\eta_{\mathrm{EPCE}} = 100\%$ and $E_{\mathrm{TX/RX}} = 1$ pJ/b. In both examples, we have assumed ideal amplifiers with $n_{\mathrm{sp}} = 1.0$. Fig. 6(b) shows the optimum number of stages m_{opt}. In Fig. 6, the fiber attenuation is 0.2 dB/km.

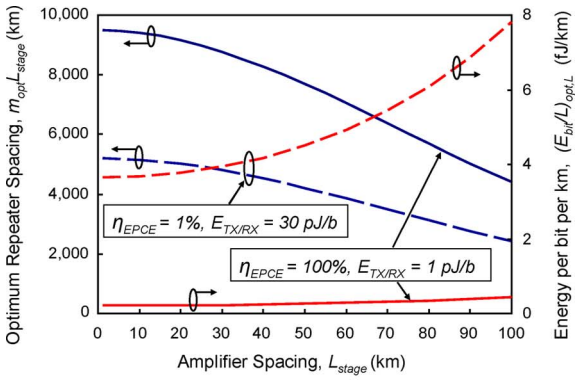

(a)

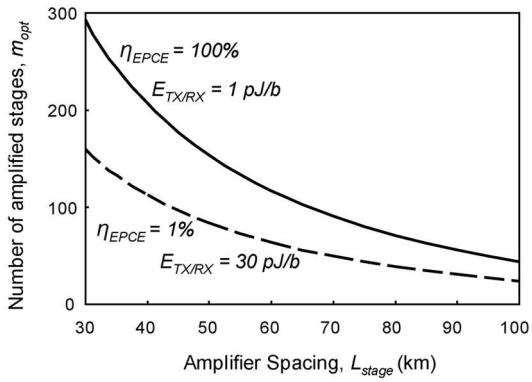

(b)

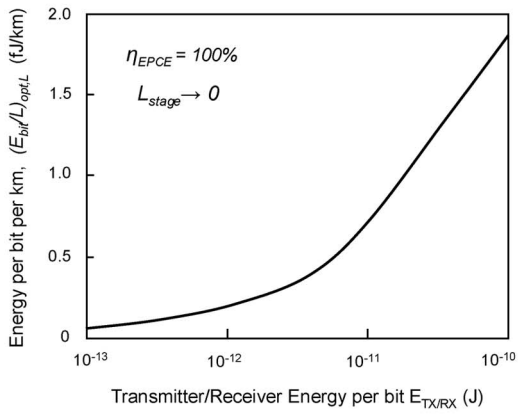

(c)

Fig. 6. (a) Optimum repeater spacing $m_{\mathrm{opt}}L_{\mathrm{stage}}$ and optimum energy per bit per kilometer against amplifier spacing L_{stage}. (b) Optimum number of amplified stages m_{opt} against amplifier spacing L_{stage}. (c) Optimum energy per bit per kilometer for distributed amplification. In all examples, $n_{\mathrm{sp}} = 1.0$, $\mathrm{SNR}_{\mathrm{bit}} = 16.1$ dB, and $\alpha = 0.2$ dB/km.

The optimum repeater spacing in Fig. 6(a) is maximum and the optimum energy per bit per kilometer is minimum when the amplifier spacing $L_{\rm stage}$ is zero. This corresponds to a system with distributed amplification. The optimum receiver spacing is around 5200 and 9500 km in a distributed amplified system for the 2010-era technologies and the ideal future system, respectively, and drops to 2400 km and 4400 with lumped amplifiers when the spacing between amplifiers is 100 km. The energy per bit per kilometer for the 2010-era system increases from 3.7 fJ/b/km for distributed amplification to 7.9 fJ/b/km with $L_{\rm stage} = 100$ km and increases from 0.2 to 0.5 fJ/b/km for the ideal future system over the same range of values of $L_{\rm stage}$.

Fig. 6(c) shows the optimum energy per bit per kilometer for a distributed amplifier from (14) as a function of the transmitter and receiver energy per bit $E_{\rm TX/RX}$ for $E_{\rm TX/RX}$ in the range of 0.1–100 pJ. In this region, the energy per bit per kilometer is in the range 0.1–2 fJ/b/km.

D. Summary of Section III

For clarity, we summarize here the key conclusion from Section III.

1) The total energy per bit per wavelength is the sum of the energies in the amplifiers and the transmitters and receivers in the system.
2) The energy per bit in a chain of amplifiers is given by (5).
3) The optimum energy per bit in an amplified transport system with optimum spacing of intermediate repeaters is given by (13) and (14).
4) The optimum spacing of repeaters $m_{\rm opt}L_{\rm stage}$ is obtained from (12) or Fig. 6.
5) If the repeater spacing is significantly less than $m_{\rm opt}L_{\rm stage}$ or if the total system length is less than $m_{\rm opt}L_{\rm stage}$, then the total energy consumption per bit in the system is dominated by the transmitters and receivers (and repeaters if they are used).
6) If the repeater spacing is significantly larger than $m_{\rm opt}L_{\rm stage}$ or if a repeaterless system has a total length larger than $m_{\rm opt}L_{\rm stage}$, then the total energy consumption per bit is dominated by the amplifiers.

Finally, it is important to stress that the data presented in Section III are lower bounds derived from an ideal system model. Today's commercial systems (see Table I) consume more energy than these data suggest. Important reasons for the differences between these ideal energy consumption figures and the energy consumption in commercial systems are discussed in Section V.

IV. Energy Consumption in Optical Transmitters and Receivers

We now consider the energy consumption in optical transmitters and receivers. Fig. 7 shows the key elements of three common types of optical transmitter. The transmitter in Fig. 7(a) uses a directly modulated laser and the transmitters in Fig. 7(b) and (c) use externally modulated lasers. All of the transmitters in Fig. 7 employ a high-speed driver or drivers and a multiplexer (MUX) that combines a number of lower bit rate signals into one high-bit-rate stream.

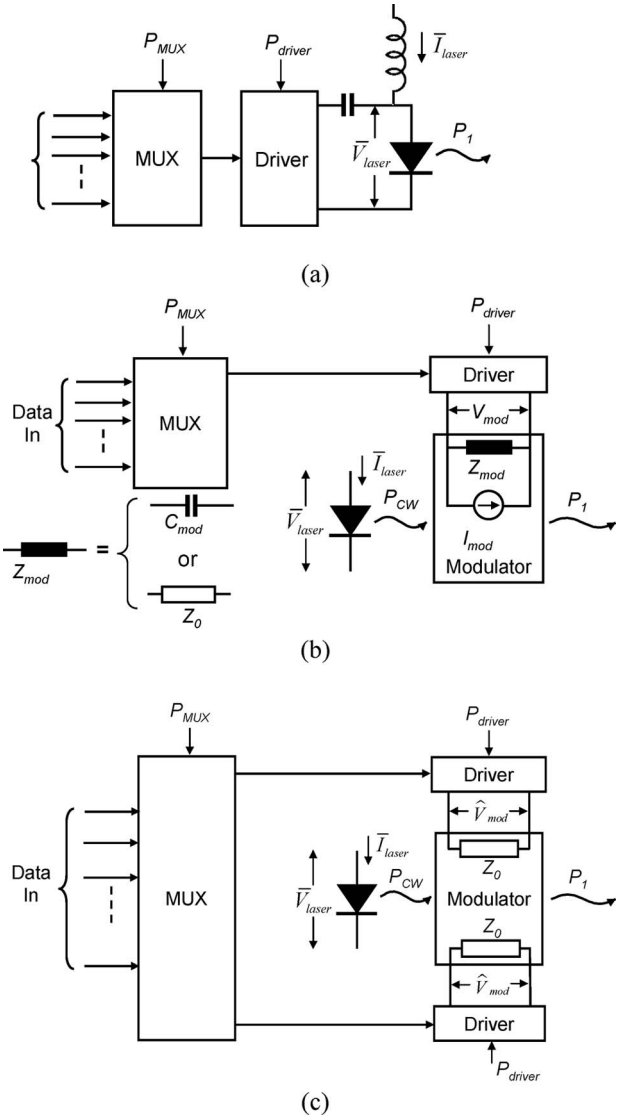

Fig. 7. Three common optical transmitters. (a) Directly modulated laser. (b) Externally modulated laser using EA modulator. (c) Externally modulated laser using E-O modulator.

A. Directly Modulated Transmitters

Because of the deleterious consequences of chirp, directly modulated lasers are generally more suitable for applications in low-bit-rate systems and interconnects [20] rather than in long-reach telecommunications. However, as shown in the following paragraphs, directly modulated lasers are potentially more energy-efficient than externally modulated transmitters. We include directly modulated lasers here as a comparison point for externally modulated lasers.

As shown in Fig. 7(a), the laser bias current and the drive signal for the directly modulated laser are combined in a bias tee (which comprises a dc blocking capacitor and an inductor). The power consumption of the MUX in Fig. 7(a) is $P_{\rm MUX}$ and the power consumption of the driver is $P_{\rm driver}$. Because the laser voltage is approximately constant, the average power consumption of the laser is approximately $\bar{V}_{\rm laser}\bar{I}_{\rm laser}$, where $\bar{V}_{\rm laser}$

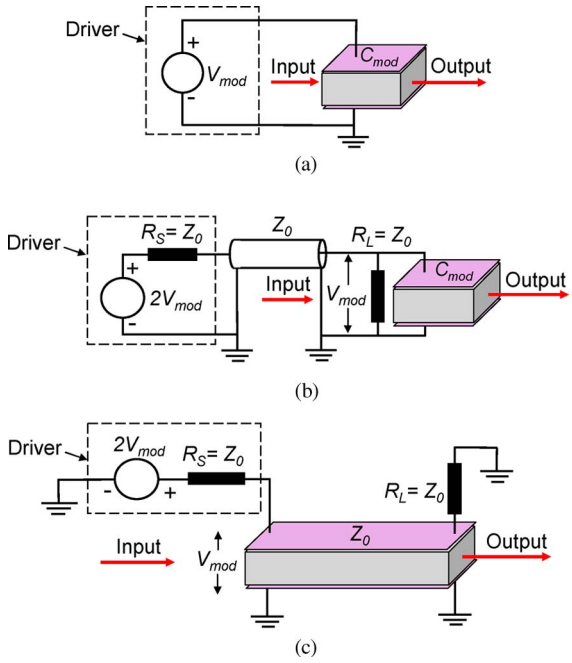

Fig. 8. Modulator structures. (a) Lumped modulator fed by low-impedance source. (b) Lumped modulator fed via transmission line. (c) Traveling-wave modulator.

and $\bar{I}_{\rm laser}$ are the average laser voltage and current, respectively. Therefore, the total power consumption $P_{\rm direct}$ of the directly modulated transmitter in Fig. 7(a) is as follows:

$$P_{\rm direct} = P_{\rm MUX} + P_{\rm driver} + \bar{V}_{\rm laser}\bar{I}_{\rm laser}. \tag{15}$$

B. Electroabsorption Modulators

The externally modulated transmitter in Fig. 7(b) employs an electroabsorption (EA) device that is driven with an instantaneous voltage of $V_{\rm mod}$. The EA modulator has an excess optical loss $L_{\rm mod}$. The input impedance of the modulator, as seen by the driver is Z. The details of this impedance depend on the type of modulator, and affect the design of the driver and the interface between the driver and the modulator. As shown in the following paragraphs, these impedance matching considerations can influence the energy consumption of the modulator and the modulation speed.

Two common types of EA modulator are illustrated in Fig. 8. Fig. 8(a) and (b) show lumped modulators and Fig. 8(c) shows a traveling-wave modulator. In lumped devices, the length of the active region is relatively short (typically around 100 μm) [21]. The impedance of the modulator $Z_{\rm mod}$, as seen by the driver can be modeled as a capacitance $C_{\rm mod}$, as shown in Fig. 7(b).

Included in Fig. 8 is a simple circuit model of the driver. If the modulator is driven by a low-impedance driver circuit [modeled as an ideal voltage source in Fig. 8(a)], the modulator can, in principle, operate at high speed because the very low resistance R of the ideal voltage source ensures a small $RC_{\rm mod}$ product. However, to achieve this, it is necessary to locate the output stage of the low-impedance driver physically very close to the modulator. A wire of any significant length connecting the two devices will introduce inductance and capacitance that can seriously degrade performance. This can become an issue if the driver and modulator are fabricated on separate chips and the structure of the chips forces a significant physical separation.

One approach for solving the physical separation problem is to interconnect the modulator to the driver using a matched transmission line, as shown in Fig. 8(b). The transmission line has characteristic impedance Z_0, which is typically 50 Ω. The driver has an internal source resistance R_S, which matches Z_0, and the modulator is shunted with a load resistance R_L, which is also equal to Z_0. Provided that the modulator capacitance $C_{\rm mod}$ is sufficiently small, the load termination on the transmission line is dominated by the resistance R_L. By matching the source and termination to the transmission line in this way, reflections are minimized and the frequency response of the device is optimized. Note that the impedance seen by the modulator is R_L in shunt with Z_0, i.e., $Z_0/2$. The *RC* product at the modulator is, therefore, $C_{\rm mod}Z_0/2$.

The input impedance $Z_{\rm mod}$ to the transmission line, as seen by the driver is Z_0. As shown in Fig. 8(b), the Thévenin equivalent source voltage needed to drive the modulator is $2V_{\rm mod}$. As a consequence of this increased voltage and the energy dissipation in the load resistor R_L in Fig. 8(b), the circuit in Fig. 8(b) is inherently less energy efficient than Fig. 8(a). A compromise solution is to omit the load resistor R_L. This results in reduced energy dissipation, but electrical reflections are increased and the *RC* product is increased by a factor of two.

Fig. 8(c) shows a schematic of a traveling-wave modulator [22], [23], incorporating an electrical transmission line of characteristic impedance Z_0, which is also typically 50 Ω. The matched driver in Fig. 8(c) is identical to Fig. 8(b). Because of their greater length, traveling-wave EA modulators tend to have lower switching voltages than lumped devices. Like Fig. 8(b) and (c) is generally less energy efficient than Fig. 8(a). However, if the switching voltage is sufficiently small in a distributed modulator, this can offset the energy impact of the load resistor.

The model of the electrical port of the EA modulator in Fig. 7(b) includes a current generator in shunt with the modulator input impedance $Z_{\rm mod}$. This current generator has instantaneous amplitude $I_{\rm mod}$, as shown in Fig. 7(b). This current generator models the current associated with photocarriers that are extracted from the active region of the device.

We assume ideal driver amplifiers that deliver all of the driver supply power $P_{\rm driver}$ in Fig. 7 to the ideal voltage source in the driver models in Fig. 8. This assumption is good for distributed amplifiers [24], but is less accurate in lumped amplifiers. Under this ideal assumption, the total power consumption of the externally modulated transmitter is as follows:

$$P_{\rm external} = P_{\rm MUX} + P_{\rm driver} + \overline{V}_{\rm laser}\overline{I}_{\rm laser} + L_{\rm mod}P_{\rm CW} \tag{16}$$

where

$$P_{\rm driver} = \overline{V_{\rm mod}I_{\rm mod}} + \frac{1}{2}C_{\rm mod}\left(V_{\rm mod}^{p-p}\right)^2 B_r \tag{17a}$$

$$P_{\rm driver} = \overline{V_{\rm mod}I_{\rm mod}} + 2\widehat{V}_{\rm mod}^2/Z_0. \tag{17b}$$

Note that the form of (17) depends on the circuit configuration of the modulator. Equation (17a) applies to Fig. 8(a) and

(17b) applies to Fig. 8(b) and (c). In (17), we have assumed a binary (i.e., two-level) digital drive voltage $V_{\rm mod}$. In Section VI, we will generalize these results to include multilevel drive signals. Note that an ideal driver amplifier with a matched 50-Ω output resistance has an ideal power conversion efficiency $\eta_{\rm driver}$ of 50%. This is because half of the supply power $P_{\rm driver}$ is dissipated in the internal resistance R_s [see Fig. 8(b) and(c)]. On the other hand, an ideal low-impedance driver has an ideal power conversion efficiency $\eta_{\rm driver}$ of 100% because there are no losses internal to the amplifier.

In (17), $V_{\rm mod}^{p-p}$ is the peak-to-peak swing of the modulation voltage, $\widehat{V}_{\rm mod}$ is the rms modulation voltage, $P_{\rm CW}$ is the laser continuous wave (CW) output power, B_r is the modulation bit rate, and $\overline{V_{\rm mod} I_{\rm mod}}$ is the average power associated with the photocurrent $I_{\rm mod}$. In essence, $\overline{V_{\rm mod} I_{\rm mod}}$ is the power required to extract photocarriers from the modulator. The $^1\!/_2 C_{\rm mod}\left(V_{\rm mod}^{p-p}\right)^2$ term in (17) represents the energy required to charge the lumped modulator capacitance $C_{\rm mod}$ per signal level transition and the $2\,\widehat{V}_{\rm mod}^2/Z_0$ term represents the power dissipated in the source and load resistances R_S and R_L in Fig. 8(b) and (c). Strictly speaking, (17b) should also include a $^1\!/_2 C_{\rm mod}\left(V_{\rm mod}^{p-p}\right)^2 B_r$ term, when applied to Fig. 8(b). However, if the $Z_0 C_{\rm mod}$ product is less than about unity, the $2\,\widehat{V}_{\rm mod}^2/Z_0$ term dominates. On average, there is one transition per bit in return-to-zero data and less than one transition per bit on non-return to zero (NRZ) data. Therefore, the second term on the right-hand side (RHS) of (17) slightly overestimates the power consumption for NRZ data.

C. Electrooptic Modulators

Fig. 7(c) shows a high-speed externally modulated transmitter using a modulator based on an induced phase shift in an optical waveguide based on the electrooptic (E-O) effect [25]. These modulators include devices using E-O materials, such as lithium niobate and silicon p-n junctions [26] operating in the depletion mode. In general, E-O modulators incorporate multiple electrical drive ports. Fig. 7(c) shows an example with two drive ports. This is typical of a NRZ DPSK transmitter. However, for more advanced modulation formats, such as RZ DPQSK, modulator structures with as many as six 50-Ω electrical drive ports are required.

High-speed E-O modulators are typically traveling-wave devices with internal resistive terminations, as shown in Fig. 8(c) [27]. However, recent work on microring-based silicon modulators [28] has opened up the possibility of high-speed lumped E-O modulation. As with traveling-wave EA modulators, the resistive termination in traveling-wave E-O devices is typically 50 Ω. The transmission line in Fig. 8(c) is shown as having parallel strip conductors for simplicity, but coplanar waveguide transmission lines are often used in planar E-O devices. The power consumption $P_{\rm external}$ of the externally-modulated transmitter in Fig. 8(c) is as follows:

$$P_{\rm external} = P_{\rm MUX} + r\,P_{\rm driver} + \overline{V}_{\rm laser}\overline{I}_{\rm laser} + L_{\rm mod}\,P_{\rm CW} \tag{18}$$

TABLE II
ENERGY CONSUMPTION IN OPTICAL TRANSMITTERS

Transmitter Type	Component		Energy per Bit: 2010-era technology (40 Gb/s)	Energy per Bit: 2020-era Target (100 Gb/s)
	MUX		10 pJ	2 pJ
Directly Modulated Fig. 6(a)	Laser ($\overline{V}_{laser}\overline{I}_{laser}$)		358 fJ	10 fJ
	Driver (P_{driver}/B_r)		212 fJ	20 fJ
	Laser + Driver		570 fJ	30 fJ
Externally Modulated (Electro-Absorption) Fig. 5(b)	Laser ($\overline{V}_{laser}\overline{I}_{laser}/B_r$)		1.5 pJ	500 fJ
	Lumped V_{mod} = 3 V	$^1\!/_2 C_{mod}(V_{mod}^{p-p})^2$	800 fJ	50 fJ
		$2\widehat{V}_{mod}^2/Z_0B_r$	4 pJ	1.6 pJ
		$\overline{V_{mod}I_{mod}}/B_r$	1.5 pJ	600 fJ
	TW V_{mod} = 1 V	$2\widehat{V}_{mod}^2/Z_0B_r$	440 fJ	176 fJ
		$\overline{V_{mod}I_{mod}}/B_r$	500 fJ	200 fJ
	Driver (P_{driver}/B_r)		25 pJ	100 fJ (C_{mod}) 3 pJ (Z_0)
	Laser + Driver		27 pJ	600 fJ (C_{mod}) 3.5 pJ (Z_0)
Externally Modulated (Electro-Optic) Fig. 5(c) V_{mod} = 3V	Laser ($\overline{V}_{laser}\overline{I}_{laser}/B_r$)		1.5 pJ	500 fJ
	$2\widehat{V}_{mod}^2/Z_0B_r$		4 pJ	1.6 pJ
	Driver (P_{driver}/B_r)		25 pJ	3 pJ
	Laser + 4 Drivers		~ 100 pJ	12 pJ

where r is the number of electrical drive ports and

$$P_{\rm driver} = \frac{\widehat{V}_{\rm mod}^2}{Z_0} \tag{19}$$

where $\widehat{V}_{\rm mod}$ is the rms modulation voltage.

D. Examples of Transmitter Energy Consumption

Table II provides some examples of energy consumption per bit in the three types of transmitter illustrated in Fig. 7. The data are presented for representative examples of 2010-era technology. In addition, under the heading "target," energy figures are presented for representative future device performance that may be achievable through aggressive improvements in technology over the next 10–15 years. These target figures are speculative, but help to identify the kinds of improvements in energy consumption that may be achievable in the 2020–2025 timeframe. The bit rate is taken to be 40 Gb/s for 2010-era technology and 100 Gb/s for the "target" column. It is possible that some devices will operate at bit rates above 100 Gb/s in the 2020–2025 timeframe. At higher bit rates, the energy per bit figures may be similar to or somewhat higher than at 100 Gb/s.

1) Electronics: The data in Table II include estimates of energy consumption of the key electronic circuits in transmitters: MUXs and drivers. In making these estimates, it is important to recognize the differences between state-of-the-art laboratory results and commercial product designs. State-of-the-art laboratory results often push devices to the limit of voltage and temperature. On the other hand, commercial products need to incorporate large safety margins on device operating conditions.

Whilst speculative, the 2020 figures are not unrealistic given the performance of laboratory devices today. For example, recent demonstrations of an 8:1 MUX using 130-nm SiGe bipolar-CMOS (BiCMOS) technology showed an energy consumption of 10 pJ/b at a bit rate of 87 Gb/s [29], and an integrated 100-Gb/s transmitter module using InP double-HBT (DHBT) consumed 15 pJ/b [30]. In contrast, a commercial 4:1 MUX [31] consumes 60 pJ/b at an aggregate bit rate of 60 Gb/s. Note that a full comparison of MUX technologies needs to take into account the MUX ratio because it is not only the very high speed stages that consume dissipated power. For example, a 40-Gb/s 4:1 MUX [32] dissipates only 0.33 W, while a 16:1 MUX [32] (including an SFI-5 framer interface) dissipates 2.8 W.

In Table II, we have selected an intermediate figure of 10 pJ/b for 2010-era technology at 40 Gb/s. In this context, we note that it is expected that the energy consumption for next generation 100-Gb/s BiCMOS [30] MUX/demultiplexer (DEMUX) chipsets could be around 20 pJ/b [32]. High-speed electronic device technologies are improving rapidly and it is not unreasonable to anticipate that with future generations of silicon–germanium (SiGe) technology that the energy consumption of high-speed MUXs could be reduced to around 2–5 pJ/b. We use a 2-pJ/b figure in Table II for the "target" energy consumption for future MUX devices operating at 100 Gb/s.

In many current-day commercial optical transmitters and in state-of-the-art laboratory demonstrations of advanced transmitter circuits, the electronic drivers are often conventional commercial RF amplifier with 50-Ω coaxial inputs and outputs terminations. This kind of amplifier is convenient for laboratory demonstrations, but is not necessarily the most energy-efficient solution. For example, the most energy-efficient circuit for an externally modulated transmitter with a lumped modulator would be a low-impedance driver (ideally $\ll 50\ \Omega$) located in very close proximity to the modulator [see Fig. 8(a)].

A typical state-of-the-art wideband driver for 40 Gb/s systems, capable of delivering voltage swings of up to around 6 V into a 50-Ω load [31] consumes about 2 W of supply power, or about 50 pJ/b, which is much larger than either the laser or the modulator. (Note that the energy consumed by the modulator is supplied by the driver, so the driver energy can never be smaller than the modulator energy). There is scope for considerable reduction in this energy using advanced circuit designs, such as distributed amplifiers. For example, a 180-nm CMOS distributed amplifier with an output voltage swing of 1.6 V into 50 Ω has been demonstrated at 40 Gb/s, with an energy consumption of 6.5 pJ/b [24] and a 50-Ω driver amplifier energy consumption of 5 pJ/b is reported in [30] for a 100-Gb/s driver using DHBT technology. In Table II, we have chosen 25 pJ/b as representative of the energy consumption of today's drivers.

Projecting into the future, the energy consumption of drivers designed to drive 50-Ω loads will ultimately be limited by the output voltage swing and the power conversion efficiency $\eta_{\rm driver}$ of the circuit. For example, a Class A driver amplifier incorporating a 50-Ω internal load and delivering a 3-V peak-to-peak output voltage swing (dc coupled) into a 50-Ω load with an efficiency $\eta_{\rm driver}$ of 35% efficiency would consume around 600 fJ/b at 100 Gb/s. This is the basis for our "target" figure in Table II for driver energy.

For lumped EA modulators with low-impedance drivers, we estimate the driver energy to be 100 fJ in the "target" column. This is twice the $1/2 C_{\rm mod}(V_{\rm mod}^{p-p})^2$ energy for the modulator assuming a driver power conversion efficiency of 50%.

2) Directly Modulated Lasers: Vertical-cavity lasers (VCSELs) have been reported with an energy consumption per bit of 358 fJ at 35 Gb/s [33]. The most energy-efficient drive source for a semiconductor laser is an amplifier with an output stage that provides a current drive directly to the laser, which is a low-impedance device. To minimize energy consumption, the output stage should be integrated closely with the laser, with no transmission line or 50-Ω resistors in the circuit. In [33], the laser is biased at around 5 mA and the current swing of the modulation signal at the laser is approximately 10 mA peak-to-peak. If the output stage of an ideal current driver has a supply voltage of 4 V, this would provide a voltage drop of 2 V across the output transistor and 2 V across the laser. The power consumption of the final stage of the driver and the laser would, therefore, be around 25 mW, or 570 fJ/b, and 358 fJ of this energy is consumed by the laser and the remaining 212 fJ is dissipated in the final stage of the driver, as shown in Table II.

In a comprehensive exploration of device requirements for interconnects, Miller [20] discusses the possibility of reducing the energy per bit in directly modulated lasers to the 10-fJ range. As pointed out in [20], nanocavity light emitters may have potential here. Many challenges remain in the fabrication of nanocavity light emitters, but recent theoretical studies have suggested that modulation bandwidths of the order of 100 GHz may be achievable at energies below 10 fJ/b [34].

3) Externally Modulated Lasers: The data in Table II for externally modulated transmitters is based on a typical telecommunications grade DFB laser, with a threshold current of 10 mA and a slope efficiency of 0.2 A/W. The laser is biased at $\overline{I}_{\rm laser} = 30$ mA and $\overline{V}_{\rm laser} = 2$ V, and with an optical output power of $P_{\rm CW} = 4$ mW. At a bit rate of 40 Gb/s, this corresponds to an energy per bit of 1.5 pJ, and at 100 Gb/s the energy is 600 fJ/b.

For a lumped EA modulator operating at 40 Gb/s, and a device capacitance of 180 fF and a modulation voltage swing of around 3 V [21], the $1/2 C_{\rm mod}\left(V_{\rm mod}^{p-p}\right)^2$ term is 800 fJ/b and the $\overline{V_{\rm mod} I_{\rm mod}}/B_r$ term is 1.5 pJ/b. This latter contribution to energy consumption is comparable with the other contributions and is larger than the $1/2 C_{\rm mod}\left(V_{\rm mod}^{p-p}\right)^2$ term. This $\overline{V_{\rm mod} I_{\rm mod}}/B_r$ term is clearly an important contributor to the total energy consumption, but is often ignored in the literature.

For a lumped modulator fed by a terminated 50-Ω transmission line, the $2\,\widehat{V}_{\rm mod}^2/Z_0 B_r$ term is 4 pJ at 40 Gb/s and 1.6 pJ at 100 Gb/s (depending on the details of the bias circuitry used). The contribution of this term is the same for the E-O modulator with $V_{\rm mod} = 3$ V.

For a traveling-wave E-O modulator with a modulation voltage swing of 1 V, the energy dissipated in the resistive termination is 440 and 176 fJ/b at 40 and 100 Gb/s, respectively, and the $\overline{V_{\rm mod} I_{\rm mod}}/B_r$ energy is approximately 500 and 200 fJ/b at these modulation rates. The least energy-efficient EA modulator is a lumped modulator fed by a terminated transmission

line. In this modulator, the total modulator energy (4.5 pJ/b) is significantly larger than the laser energy (1.5 pJ/b).

There is some scope for future improvement in modulator energy per bit for EA and E-O modulators, as indicated in the "target" column of Table II. For lumped modulators fed by low-impedance drivers, the energy consumption can be reduced by reducing the device capacitance and reducing the voltage. Recently, device capacitances as low as 11 fF with 3 V switching voltages have been reported [35], which corresponds to a $\frac{1}{2}C_{\rm mod}\left(V_{\rm mod}^{p-p}\right)^2$ term of 50 fF/b. There will be challenges in interfacing low-impedance driver amplifier to such a device, but we use this 50 fJ/b figure as our "target" for the $\frac{1}{2}C_{\rm mod}\left(V_{\rm mod}^{p-p}\right)^2$ term under the expectation that this will be possible by 2020. Nevertheless, as shown in Table II, the $\overline{V_{\rm mod}I_{\rm mod}}/B_r$ term (600 fF/b) dominates over the $\frac{1}{2}C_{\rm mod}\left(V_{\rm mod}^{p-p}\right)^2$ term (50 fJ/b) for a device with a switching voltage of $V_{\rm mod} = 3$ V. This suggests that, depending on the optical power level being used, future efforts to reduce the energy consumption of lumped modulators may be better directed at reducing the switching voltage than at further reducing the device capacitance.

In estimating the "target" energy for traveling-wave modulators, we note that in principle the energy consumption could be reduced by increasing the characteristic impedance of the transmission line. But there is an upper limit on the characteristic impedance because increased characteristic impedance would tend to reduce the electric field in the active region associated with the modulation voltage. For these reasons, the target figures for the $\frac{1}{2}C_{\rm mod}(V_{\rm mod}^{p-p})^2$ and $2\,\widehat{V}_{\rm mod}^2/Z_0B_r$ terms of Table II represent only modest improvements on 2010-era technology.

The data in Table II for externally modulated transmitters using E-O modulators uses the same laser as for the EA modulator. The modulation voltage swing $V_{\rm mod}$ in E-O modulators is typically around 3 V. Like the EA modulator, the "target" figure for the $\widehat{V}_{\rm mod}^2/Z_0$ term represents only a modest improvement on 2010-era technology.

E. Optical Receivers

Fig. 9 shows circuit diagrams of three optical receiver configurations. Fig. 9(a) and (c) are single-ended receivers and Fig. 9(b) is a balanced receiver. The photodiodes in Fig. 9(a) and (b) are connected to a transmission line with characteristic impedance Z_0 (typically 50 Ω) and are shunted with an impedance-matching resistor R_S. The transmission line in Fig. 9(a) and (b) is terminated at the input of an electronic clock and data recovery (CDR) and DEMUX circuit with a matched input resistance $R_{\rm in} = Z_0$. The CDR/DEMUX circuit may also include A/D converters (ADCs). The configurations in Fig. 9(a) and (b) enable the photodiode(s) to be located some distance from the electronic components and to use a low-loss transmission line to convey the detected signal to the electronic circuitry.

The receiver circuit in Fig. 9(c) has no transmission line and the photodiode is located in close proximity to the amplifier [36]. This amplifier is typically a low-input-impedance transimpedance amplifier (TIA). The input resistance $R_{\rm in}$ of this

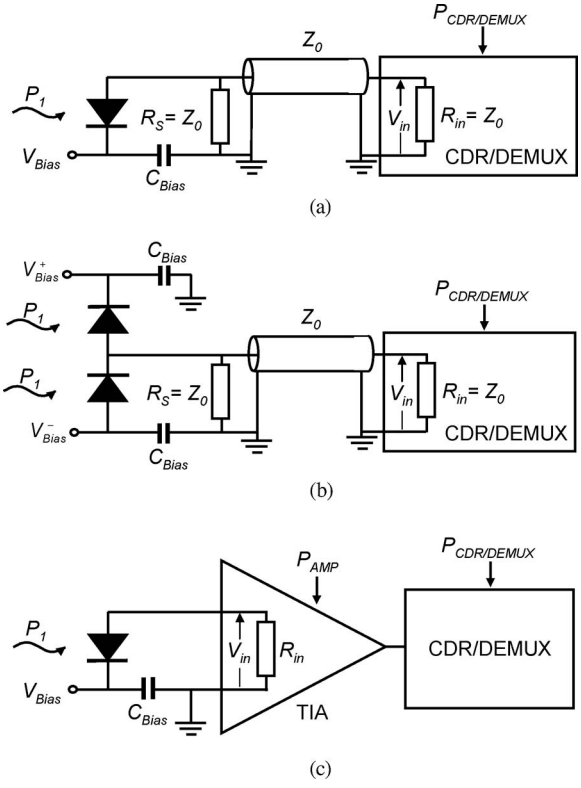

Fig. 9. Photodiode and bias circuitry of receiver front ends. (a) Single-ended with transmission line connecting photodiode to CDR/DEMUX. (b) Balanced with transmission line connecting photodiode to CDR/DEMUX. An optical preamplifier (not shown) boosts the input optical power levels in (a) and (b). (c) Single-ended with TIA and CDR/DEMUX.

amplifier is ideally $\ll 50\ \Omega$ because this helps to minimize the *RC* product and maximize bandwidth. The signal input voltage to the electronic DEMUXs in Fig. 9 is $V_{\rm in}$.

The photodiodes in Fig. 9 are all reverse-biased with a voltage $V_{\rm Bias}$. If an EDFA preamplifier (not shown in Fig. 9) is employed in front of the receivers in Fig. 9(a) and (b), it is possible to achieve an input voltage swing $V_{\rm in}^{p-p}$ of the order of 0.5–1 V.[1] This signal level is generally adequate to directly drive a DEMUX or other circuitry [37], [38], thereby eliminating the need for a preamplifier. In receivers that incorporate an electronic TIA [see Fig. 9(c)], an EDFA preamplifier may not be required. The power consumption of the CR/DEMUX in Fig. 9 is $P_{\rm CDR/DEMUX}$ and the power consumption of the electronic TIA in Fig. 9(c) is $P_{\rm AMP}$.

If the responsivity of the photodiodes in Fig. 9 is $\Re$, the power supplied by the bias circuit is as follows:

$$P_{\rm Bias} = \Re V_{\rm Bias}\left(\overline{P_1} + \overline{P_2}\right) \tag{20}$$

where $\overline{P_1}$ and $\overline{P_2}$ are the mean optical input powers incident on the photodiodes. The peak-to-peak voltage swing $V_{\rm in}^{p-p}$ is as follows:

$$V_{\rm in}^{p-p} = \frac{R_{\rm in}\Re(P_1^{p-p} + P_2^{p-p})}{2}. \tag{21}$$

[1]This mode of operation requires photodiodes with a high-damage threshold.

where P_1^{p-p} and P_2^{p-p} are the peak-to-peak optical power swings incident on the photodiodes.

If $\overline{P_1} = P_1^{p-p}/2$ and $\overline{P_2} = P_2^{p-p}/2$, it follows that

$$P_{\mathrm{Bias}} = \frac{V_{\mathrm{Bias}} V_{\mathrm{in}}^{p-p}}{R_{\mathrm{in}}} \tag{22}$$

$$V_{\mathrm{in}}^{p-p} = \Re R_{\mathrm{in}}(\overline{P_1} + \overline{P_2}). \tag{23}$$

Note that for Fig. 9(a) and (c), P_2^{p-p} in (21) and $\overline{P_2}$ in (23) are set to zero.

The total power consumption P_{total} of the optical receiver (excluding the power consumption of the CDR/DEMUX) is as follows:

$$\begin{aligned} P_{\mathrm{total}} &= P_{\mathrm{Bias}} + P_{\mathrm{preamp}} + P_{\mathrm{AMP}} \\ &= \frac{V_{\mathrm{in}}^{p-p}}{R_{\mathrm{in}}}\left[V_{\mathrm{Bias}} + \frac{1}{\eta_{\mathrm{preamp}}\Re}\right] + P_{\mathrm{AMP}} \end{aligned} \tag{24}$$

where $P_{\mathrm{preamp}} = (\overline{P_1} + \overline{P_2})/\eta_{\mathrm{preamp}}$ is the power consumed by the EDFA preamplifier and η_{preamp} is the electrical power conversion efficiency of the optical preamplifier. Note that for Fig. 8(a) and (b), $P_{\mathrm{AMP}} = 0$, and for Fig. 9(c), $P_{\mathrm{preamp}} = 0$ if no optical preamplifier is used. Under these conditions, the $1/\eta_{\mathrm{preamp}}\Re$ term in (24) is set to zero.

To achieve an input peak-to-peak voltage swing V_{in}^{p-p} of 0.5 V in Fig. 9(a) and (b) with a bias voltage of 2 V, a responsivity of 0.73 A/W [38], a characteristic impedance of $Z_0 = 50\,\Omega$, and an electrical power conversion efficiency of $\eta_{\mathrm{preamp}} = 1\%$ (typical of 2010-era technology), the total input optical power is $(\overline{P_1} + \overline{P_2}) = 14$ mW and the total power consumption of the receiver is $P_{\mathrm{total}} = 1.4$ W. If the electrical power conversion efficiency of the optical preamplifier could be improved to around 10%, the power consumption of the receiver would drop to $P_{\mathrm{total}} =$ 157 mW. At a bit rate of 100 Gb/s, this corresponds to a bias circuit and preamplifier energy consumption of 1.6 pJ/b.

The receiver in Fig. 9(c) would typically be operated without an optical preamplifier and with an input optical power level that is 10–20 dB less than the 14-mW figure in the previous example. At this low-power level, the $V_{\mathrm{in}}^{p-p} V_{\mathrm{bias}}/R_{\mathrm{in}}$ term in (24) would be one to two orders of magnitude smaller, or less than 200 μW. Therefore, the power consumption of the TIA dominates the total power consumption. A typical 2010-era commercial 40-Gb/s TIA consumes approximately 145 mW (3.6 pJ/b) [39] and a laboratory demonstration of a TIA incorporating automatic gain control (AGC) and operating at 40 Gb/s in 90-nm CMOS has achieved an energy consumption as low as 1.9 pJ/b [40]. A CDR is included in the chip and consumes an additional 1.2 pJ/b [40]. Our "target" energy consumption for a TIA at 100 Gb/s is 0.5 pJ/b.

High-speed CDR/DEMUX circuits typically consume considerably more energy than MUXs because a larger proportion of the circuit operates at high speed [32]. For example, in [41], a laboratory 100 Gb/s, 1:2 InP HBT-based 1:2 DEMUX consumed 10–30 pJ/b, and in [42], an InP DHBT-based CDR integrated with a 1:2 DEMUX at 100 Gb/s consumed 21 pJ/b. DEMUX circuits with higher demultiplexing ratios (e.g., 1:4, 1:8, and 1:16) consume considerably more energy than a 1:2 DEMUX.

TABLE III
ENERGY CONSUMPTION IN OPTICAL RECEIVERS

Receiver Type	Component	Energy per Bit	
		2010-era technology (40 Gb/s)	2020-era Target (100 Gb/s)
	CDR/DEMUX	20 pJ	2 pJ
Figs 8(a) and 8(b)	Optical preamplifier power and bias power	35 pJ	1.6 pJ
Fig. 8(c)	Transimpedance amplifier power	3.6 pJ	0.5 pJ

In addition, as data are demultiplexed to lower bit rates, there are more parallel electronic channels, albeit at lower bit rates. This highlights the fact that there is considerable energy consumption in the receiver and transmitter electronics at circuit levels removed from the high-bit-rate circuits. We will address this issue in more detail in Section V.

The data in the previous paragraphs are summarized in Table III, which shows the dominant contribution to power consumption for each circuit—the optical preamplifier and bias circuit contributions in Fig. 9(a) and (b), and the TIA contribution in Fig. 9(c). In calculating the figures in Table III, we have made the fairly optimistic assumption that the power conversion efficiency of the optical preamplifier can be improved to around 25% by 2020.

V. ENERGY LOSSES AND OVERHEADS

A. Lower Bounds Compared to Energy in Commercial Systems

In Section III-B, we have shown that the lower bound on amplifier energy consumption is approximately 50 fJ/b in a 1000-km amplified system with a 100-km repeater spacing. Table II shows that the lower bound on energy in a 2010-era externally modulated laser transmitter is about 60 pJ/b (dominated by the MUX and driver). Similarly, Table III shows that the lower bound on energy consumption in a 2010-era high-speed transimpedance optical receiver is about 34 pJ/b (dominated by the CDR/DEMUX). Therefore, the lower bound of the total energy consumption for a 2010-era 1000-km system is around 90 pJ/b (dominated by the transmitter).

It is instructive to compare the lower bound figures in the previous paragraph with the energy consumption data for a typical commercial system, as shown in Table I. It turns out that the 90-pJ/b lower bound figure in the previous paragraph for a 1000-km system is about 8% of the 1.1-nJ/b energy consumption in the typical commercial systems. Similarly, the lower bound on total energy consumptions in the optical amplifiers is about 0.01% of the 600 pJ/b consumed by the amplifiers in the typical commercial system.

Why would there be such a large difference between the lower bounds obtained here and the data for commercial system? There are a number of good reasons: 1) today's optical amplifiers have power conversion efficiencies of the order of only 1% [11] and typically include a number of control and management functions that consume additional power; 2) transceivers in commercial systems include a number of additional processing circuits,

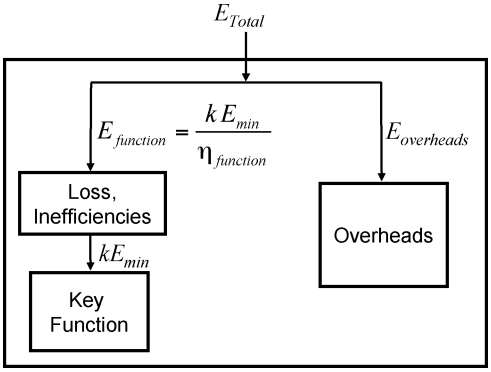

Fig. 10. Model of energy overheads in subsystem.

such as supervisory, management, and control circuitry; and 3) commercial systems available on the market do not necessarily use the latest generations of technology and keep the operating envelope of semiconductor devices well away from regions, where performance is optimized, but reliability is degraded.

B. Modeling Inefficiencies and Overheads

To model the difference between the ideal lower bound on energy consumption in a network subsystem and the energy consumption in a real subsystem, we introduce the concept of subsystem efficiency. Fig. 10 illustrates the flow of energy in a subsystem (or system). The subsystem in Fig. 10 is, in general, a WDM subsystem, operating with k wavelengths. It could be any part of a communications network, including, for example, a single optical amplifier, an amplifier chain, an optical transmitter, a receiver, or a repeater.

The total input energy per bit period $E_{\rm Total}$ into the subsystem is the sum of two components: $E_{\rm function}$ and $E_{\rm overheads}$. $E_{\rm function}$ is the energy per bit period required to perform the key active function of the subsystem and $E_{\rm overheads}$ is the energy per bit period consumed by ancillary functions that are not essential to the key function, but are required in order for the subsystem to operate. The power $P_{\rm overheads}$ consumed by the overhead ancillary functions is related to the overhead energy per bit period by $E_{\rm overheads} = P_{\rm overheads}/B_r$.

If the subsystem is an optically amplified link, $E_{\rm function}$ includes the energy consumed by the optical amplifier pump lasers. This energy increases with the optical signal level and with the number of wavelengths k. $E_{\rm overheads}$ includes the fixed energy consumed by ancillary functions, such as temperature controllers, device monitoring and operational signaling, as well as supervisory and management circuitry.

The ideal lower bound on energy required to perform the key active function of the subsystem per wavelength is $E_{\rm min}$. In practice, $E_{\rm function}$ will be larger than the ideal value of $kE_{\rm min}$ due to losses, inefficiencies, and other nonideal behavior. For example, in an optically amplified link, these include inefficiencies in the pump lasers, coupling losses, and nonunity spontaneous emission factor $n_{\rm sp}$. In addition, dispersion penalties and system margins may require the optical power level to be set at a larger value than the absolute minimum required for a specified bit rate, and sophisticated coding/decoding circuits are required if the system performance is to approach the Shannon bound. In the model in Fig. 10, this nonideal behavior is accounted for by the efficiency factor $\eta_{\rm function}$. The minimum energy $E_{\rm min}$ for the function is related to $E_{\rm function}$ by the relationship $E_{\rm function} = kE_{\rm min}/\eta_{\rm function}$.

The combined effects of the inefficiencies and the energy overheads can be encapsulated in terms of an overall subsystem efficiency parameter $\eta_{\rm subsystem}$. This parameter describes the overall efficiency of the subsystem in terms of the total input energy and the lower bound on energy for the key function, and is defined as follows:

$$\eta_{\rm subsystem} = \frac{kE_{\rm min}}{E_{\rm Total}} = \frac{1}{\eta_{\rm function}^{-1} + (P_{\rm overheads}/B_r kE_{\rm min})}. \tag{25}$$

We now return to the comparison between the theoretical lower bound $E_{\rm min}$ for optical transceivers and optically amplified links, and real-energy consumption figures for 2010-era optical amplifiers (see Table I). In commercial optical transceivers, $\eta_{\rm subsystem}$ is around 1–10%, and in commercial optical line amplifiers, $\eta_{\rm subsystem}$ is around 0.1–1%. It is difficult to estimate how much energy in commercial equipment is consumed by losses and inefficiencies, and how much is consumed by overheads because manufacturers generally do not publicly disclose information about the power consumption profile of their products. However, we estimate for typical commercial optical amplifiers operating with $k = 40$ wavelengths that $\eta_{\rm function} \sim <2\%$, and $E_{\rm function}$ and $E_{\rm overheads}$ are roughly equal in magnitude. Similarly, we estimate that in 2010-era commercial transceivers $\eta_{\rm function} <20\%$, and $E_{\rm function}$ and $E_{\rm overheads}$ are also roughly equal in magnitude.

An important conclusion is that most of the energy in current-day transport systems is consumed in losses, inefficiencies, and energy overheads. Therefore, a key strategy in reducing the energy consumption of transport systems will be to reduce energy overheads and improve other losses and inefficiencies.

VI. Modulation Formats and Energy Efficiency

Spectrally efficient modulation formats, such as DP-QPSK and QAM will play an important role in future transport systems [43]. It is therefore important to consider the impact of modulation formats on the lower bound on overall energy efficiency of transport systems. The modulation format impacts upon the energy consumption of the transmitter and receiver and also the energy consumption of the optical amplifiers. In this section, we consider the influence of modulation format on energy consumption in optical transceivers and optically amplified links.

In our analysis of the impact of modulation formats on energy efficiency, we consider the three different domains of operation identified in Section III-C. These three domains are as follows.

1) The total system length or the repeater spacing is less than $m_{\rm opt}L_{\rm stage}$. In this domain, the minimum overall energy per bit is dominated by the transmitters and receivers.

2) The repeater spacing is more than $m_{\rm opt}L_{\rm stage}$. In this domain, the minimum overall energy per bit is dominated by the optical amplifiers.
3) The total system length is equal to $m_{\rm opt}L_{\rm stage}$, or the repeater spacing is equal to $m_{\rm opt}L_{\rm stage}$. In this domain, the contribution of the transmitters and receivers to the minimum overall energy consumption is equal to the contribution of the optical amplifiers.

A. Energy Dominated by Optical Transmitters and Receivers

As shown in Section IV, two key factors influence the driver energy: the number 50-Ω electrical ports on the modulator(s) and the modulator switching voltage. Transmitters with spectrally efficient modulation formats generally require multiple modulator drive ports, thereby increasing the energy consumption. However, this increase may be offset to a degree because the symbol rate on these ports can be lower than the bit rate of the transmitter, and modulators operating at lower bit rates can be designed to operate at lower switching voltages [25].

For example, DP-QPSK, which operates with 4 bits per symbol, can be generated using a four-port modulator scheme [44]. The symbol rate of the drive signals on each of the four-modulator ports is one-quarter of the aggregate transmitted bit rate. It is possible, in principle, to use a modulator that is optimized for this lower symbol rate and operates at a lower switching voltage. Thus, depending on the modulator voltage, the lower bound on total energy per transmitted bit consumed by the modulators may less than for an OOK modulator operating at the same bit rate. Note that DP-QPSK requires four drive amplifiers, while OOK requires one drive amplifier.

To provide a concrete example of energy consumption associated with spectrally efficient modulation formats, we focus here on a QAM transmitter and receiver. This modulation format requires a coherent optical receiver, but the optical transmitter is more energy efficient than a DP-QPSK transmitter.

QAM transmitters with high-spectral efficiency can be constructed using a dual-drive modulator using the circuit configuration in Fig. 7(c) [45]. According to (19), the energy per bit required to drive the modulator is as follows:

$$E_{\rm bit,mod} = r\frac{P_{\rm driver}}{B_r} = \frac{r\widehat{V}_{\rm mod}^2}{B_r Z_0} \tag{26}$$

where $r = 2$ is the number of ports on the modulator. Note that $E_{\rm bit,mod}$ in (26) is independent of the symbol rate because B_r is equal to the symbol rate times the number of bits per symbol. There is some difference between the $\widehat{V}_{\rm mod}^2$ term in QAM and OOK or BPSK due to waveform differences between binary and multilevel modulation. However, the energy consumption of a QAM driver and modulator is about twice that of the modulator for an OOK transmitter or a BPSK transmitter.

A receiver for QAM typically employs a local oscillator, an array of balanced photodiodes (possibly combined with two TIAs) followed by two ADCs [45]. Following the analysis in Section IV-E, it is expected that the energy consumption of the receiver will be dominated by the TIAs and the ADCs. Therefore, the receiver energy consumption for QAM is larger than that of an OOK or BPSK receiver. Following this reasoning, the total transmitter/receiver energy per bit $E_{\rm TX/RX,QAM}$ in a QAM system is likely to be larger than for OOK or BPSK.

B. Energy Dominated by Optical Amplifiers

When the repeater spacing is more than $m_{\rm opt}L_{\rm stage}$, the energy consumption is dominated by the optical amplifiers. The minimum amplifier energy is given by (6) and is proportional to the SNR per bit $\rm SNR_{bit}$. This term is strongly dependent on the modulation format and increases by about 2 dB for each doubling of the constellation size M. Therefore, $\rm SNR_{bit}$ for 16-QAM is about 4 dB larger than for DPSK, and in 64-QAM, it is about 8 dB larger than for DPSK. The net result is that the energy per bit is correspondingly increased by 4 and 8 dB, respectively. The benefit obtained in return for this reduction in energy efficiency is an increase in the spectral efficiency of approximately four times or more.

C. Optimum Repeater Spacing

When the repeater spacing is optimized to minimize the overall energy consumption, the overall (optimized) energy consumption per bit per unit transmission distance is given by (13). According to (13), this optimized energy consumption is proportional to $\sqrt{\rm SNR_{bit}E_{TX/RX}}$. If, as discussed in aforementioned Section VI-A, $E_{\rm TX/RX}$ for a QAM system is about twice that for an BPSK system, then for a system with optimum repeater spacing, the energy per bit in a QAM system is approximately $\sqrt{2\ \rm SNR_{bit}}$ larger than an optimized BPSK system. From this, we deduce that in an optimized system, the energy consumption for 16-QAM would about 3.5 dB larger than for DPSK, and in 64-QAM, it would about 5.5 dB larger than for DPSK. These increases in energy consumption are indicative only and clearly depend on the actual energy consumption of the BPSK and QAM transmitter and receiver.

D. Commercial Systems

We need to stress that the results in the previous paragraphs apply to ideal systems with zero energy overheads. The results in Section VI-A–C show that at the ideal theoretical lower bound on energy in systems with high-spectral efficiency is not as low as systems with low-spectral efficiency. However, we now show that this is not necessarily the case in current commercial systems. The reason for this is that commercial systems exhibit large energy overheads.

Consider a system in which k wavelengths per fiber, each carry data at bit rate B_r. The number of fibers is f and the total number of wavelengths is $k_{\rm total} = f\cdot k$. According to (25), the total energy consumption $E_{\rm TX/RX}$ of the system per bit per wavelength is as follows:

$$\begin{aligned} E_{\rm bit} &= \frac{E_{\rm total}}{k_{\rm total}} \\ &= \frac{E_{\rm AMP\text{-}min}}{\eta_{\rm amp}} + \frac{E_{\rm TX/RX}}{\eta_{\rm TX/RX}} + \frac{B_r P_{\rm overheads,TX/RX}}{k_{\rm total}} \end{aligned}$$

$$+\frac{fB_r P_{\mathrm{overheads,AMP}}}{k_{\mathrm{total}}} \tag{27}$$

where f is the number of fibers in the system, $P_{\mathrm{overheads,TX/RX}}$ is the overhead power consumption in all optical transmitters and receivers, and $P_{\mathrm{overheads,AMP}}$ is the overhead power consumption in all optical amplifiers.

In 2010-era systems, the two overhead terms on the RHS of (27) are large. In particular, the $P_{\mathrm{overheads,AMP}}$ term on the RHS of (27) can dominate the energy consumption. Note that this term is proportional to the number of fibers because extra amplifiers are needed as additional fibers are added to the system. Therefore, minimum energy consumption is achieved by minimizing the number of fibers and amplifiers. Therefore, in today's transport systems, there is an energy-efficiency incentive to employ spectrally efficient modulation formats and to maximize the utilization of the optical fiber. If $P_{\mathrm{overheads,AMP}}$ is reduced in future generations of amplifier, or if the transmission distance is short, the $P_{\mathrm{overheads,TX/RX}}$ term can dominate in (27). Under these circumstances, from a strict energy-efficiency point of view, there is no need to achieve high spectral efficiency. As shown earlier, if the first two terms on the RHS of (27) dominate, high spectral efficiency is in fact disadvantageous from a strict energy-efficiency point of view.

VII. Discussion and Conclusion

We have identified the lower bound on energy consumption in optically amplified transport systems and have shown how this bound scales with transmission distance. The lower bound is limited by the number of optical amplifiers required in the system and their energy consumption. In turn, the number of amplifiers depends on the system length, the ASE in the optical amplifiers and by the sensitivity of the optical receiver. In determining the lower bound on energy consumption in transport systems, it is necessary to consider the energy of the optical transmitters and receivers used in the end terminals and in intermediate repeaters. While advanced modulation formats, such as QAM provide high-spectral efficiency, they are generally less energy efficient at the ideal limit than simple modulation formats, such as OOK. However, in practical 2010-era systems, with large energy overheads in the amplifiers, high-spectral efficiency can help to improve overall energy efficiency.

Aside from improvements in current-day technologies, there are two approaches that may possibly enable a reduction in the energy consumption to figures that are smaller than calculated here. One approach would be through a reduction in fiber loss, enabling fewer amplifiers to be used. The lower bound scales with the fiber loss coefficient α. Therefore, a reduction in the lower bound by an order of magnitude would require the fiber loss to be reduced from 0.2 to 0.02 dB/km. This low loss is beyond the capabilities of silica fibers.

A second approach for reducing the lower bound would be to use coding to enable the receiver sensitivity to approach the Shannon limit. However, the additional energy used in the required coding circuitry may overwhelm any benefits. Future generations of very low energy electronic devices may eventually enable coding to become a viable method for improving the energy efficiency of optical transport systems.

We have shown that overall energy consumption can be minimized by optimizing the spacing of repeaters in optically amplified systems. The optimum repeater spacing for minimum energy consumption is typically on the order of several thousands of kilometers. As technologies improve, the optimum repeater spacing for minimum energy consumption will approximately 10 000 km. For transport systems with lengths that are less than this optimum repeater spacing, it is clearly desirable to minimize the number of instances, where signals are converted between optical and electrical formats.

Because optical transmitters and receivers are limited principally by the electronic component technology used to drive the optical components, it is difficult, if not impossible, to define a fundamental lower limit on transmitter/receiver energy consumption. However, we have estimated some aggressive target figures for future transmitters and receivers.

The focus of this paper has been an analysis of the theoretical lower bounds on energy in transport systems. The difference between these ideal lower bounds and the actual energy consumption in commercial systems today can be accounted for in terms of inefficiencies and energy overheads. These arise at many levels in typical transmission systems, from inefficiencies at the device level in optical amplifier pump lasers and their cooling systems, at the circuit level in the tradeoff of efficiency for speed in high-speed electronic circuits used in transmitters and receivers, and at the system level in terms of multiplexing and management overheads. A key strategy in reducing the energy consumption of optical transport systems will be to reduce these inefficiencies and overheads.

Acknowledgment

The author would like to thank for many valuable interactions with his colleagues R. Ayre, J. Baliga, and K. Hinton and for their assistance in assembling the data for Fig. 1. The author would also like to thank M. Möller of Saarland University for his valuable comments on a draft of the manuscript and D. Miller of Stanford University, G Epps of Cisco, G. Raybon, P. Winzer, A. Chraplyvy, and X. Liu of Alcatel-Lucent, and I. Young of Intel for valuable discussions.

References

[1] R. S. Tucker, "Green optical communications—Part II: Energy limitations in networks," *IEEE J. Sel. Top. Quantum Electron.*, vol. 17, no. 2, pp. 261–274, Mar./Apr. 2011.

[2] M. Gupta and S. Singh, "Greening of the internet," presented at the ACM SIGCOMM, Karlsruhe, Germany, 2003.

[3] R. S. Tucker, R. Parthiban, J. Baliga, K. Hinton, R. W. A. Ayre, and W. V. Sorin, "Evolution of WDM optical IP networks: A cost and energy perspective," *J. Lightw. Technol.*, vol. 27, no. 3, pp. 243–252, Feb. 2009.

[4] J. Baliga, R. Ayre, K. Hinton, W. V. Sorin, and R. S. Tucker, "Energy consumption in optical IP networks," *J. Lightw. Technol.*, vol. 27, no. 13, pp. 2391–2403, Jul. 2009.

[5] S. Han, "Moore's law and energy and operations savings in the evolution of optical transport platforms," *IEEE Commun. Mag.*, vol. 48, no. 2, pp. 66–69, Feb. 2010.

[6] Fujitsu Data Sheets. (2010). [Online]. Available: http://www.fujitsu.com

[7] Finisar. (2008). Tunable DPSK optical module product brief. [Online]. Available: www.finisar.com

[8] E. B. Desurvire, "Capacity demand and technology challenges for lightwave systems in the next two decades," *J. Lightw. Technol.*, vol. 24, no. 12, pp. 4697–4710, Dec. 2006.

[9] R.-J. Essiambre, G. Kramer, P. Winzer, G. J. Foschini, and B. Goebel, "Capacity limits of optical fiber networks," *J. Lightw. Technol.*, vol. 28, no. 4, pp. 662–701, Feb. 2010.
[10] Network and Telecom Equipment—Energy and Performance Assessment. (2010). ECR Initiative. [Online]. Available: http://www.ecrinitiative.org/
[11] E. Desurvire, D. Bayart, B. Desthieux, and S. Bigo, *Erbuim-Doped Fiber Amplifiers: Device and System Developments*. New York: Wiley, 2002.
[12] X. Liu, S. Chandrasekhar, and A. Leven, "Self-coherent optical transport systems," in *Optical Fiber Telecommunications V, B: Systems and Networks*, I. Kaminow, T. Li, and A. Willner, Eds. Amsterdam, The Netherlands: Elsevier, 2008.
[13] M. Karlsson and E. Agrell, "Which is the most power-efficient modulation format in optical links?" *Opt. Exp.*, vol. 17, pp. 10814–10819, 2009.
[14] J. G. Proakis, *Digital Communications*, 4th ed. New York: McGraw-Hill, 2001.
[15] I. B. Djordjevic, M. Arabaci, and L. L. Minkov, "Next generation FEC for high-capacity communication in optical transport networks," *J. Lightw. Technol.*, vol. 27, no. 16, pp. 3518–3530, Aug. 2009.
[16] M. L. C. Stevens, D. O. Robinson, B. S. Boroson, D. M. Kachelmyer, and A. L. Kachelmyer, "Optical homodyne PSK demonstration of 1.5 photons per bit at 156 Mbps with rate-1/2 turbo coding," *Opt. Exp.*, vol. 16, pp. 10412–10420, 2008.
[17] H. F. Haunstein, T. Schorr, A. Zottmann, W. Sauer-Greff, and R. Urbansky, "Performance comparison of MLSE and iterative equalization in FEC systems for PMD channels with respect to implementation complexity," *J. Lightw. Technol.*, vol. 24, no. 11, pp. 4047–4054, Nov. 2006.
[18] Core Optics Ultra-FEC Chip. [Online]. Available: http://www.coreoptics.com/
[19] R. S. Tucker, "The role of optics and electronics in high-capacity routers," *J. Lightw. Technol.*, vol. 24, no. 12, pp. 4655–4673, Dec. 2006.
[20] D. A. B. Miller, "Device requirements for optical interconnects to silicon chips," *Proc. IEEE*, vol. 97, no. 7, pp. 1166–1185, Jul. 2009.
[21] C. Yuanbing, P. Jiaoqing, W. Yang, Z. Fan, W. Baojun, Z. Lingjuan, Z. Hongliang, and W. Wei, "40-Gb/s low chirp electroabsorption modulator integrated with DFB laser," *IEEE Photon. Technol. Lett.*, vol. 21, no. 6, pp. 356–358, Mar. 2009.
[22] C. Z. Zhang, C. Yi-Jen, P. Abraham, and J. E. Bowers, "25 GHz polarization-insensitive electroabsorption modulators with traveling-wave electrodes," *IEEE Photon. Technol. Lett.*, vol. 11, no. 2, pp. 191–193, Feb. 1999.
[23] J. W. Shi, C. A. Hsieh, A. C. Shiao, Y. S. Wu, F. H. Huang, S. H. Chen, Y. T. Tsai, and J. I. Chyi, "Demonstration of a dual-depletion-region electroabsorption modulator at 1.55-μm wavelength for high-speed and low-driving-voltage performance," *IEEE Photon. Technol. Lett.*, vol. 17, no. 10, pp. 2068–2070, Oct. 2005.
[24] J.-C. Chien and L.-H. Lu, "40-Gb/s High-Gain distributed amplifiers with cascaded gain stages in 0.18-micrometer CMOS," *IEEE J. Solid-State Circuits*, vol. 42, no. 12, pp. 2715–2725, Dec. 2007.
[25] E. L. Wooten, K. M. Kissa, A. Yi-Yan, E. J. Murphy, D. A. Lafaw, P. F. Hallemeier, D. Maack, D. V. Attanasio, D. J. Fritz, G. J. McBrien, and D. E. Bossi, "A review of lithium niobate modulators for fiber-optic communications systems," *IEEE J. Sel. Top. Quantum Electron.*, vol. 6, no. 1, pp. 69–82, Jan./Feb. 2000.
[26] M. R. Watts, W. A. Zortman, D. C. Trotter, R. W. Young, and A. L. Lentine, "Low-voltage, compact, depletion-mode, silicon Mach–Zehnder modulator," *IEEE J. Sel. Top. Quantum Electron.*, vol. 16, no. 1, pp. 159–164, Jan./Feb. 2010.
[27] T. Kawanishi, T. Sakamoto, A. Chiba, M. Izutsu, K. Higuma, J. Ichikawa, T. Lee, and V. Filsinger, "High-speed dual-parallel Mach-Zehnder modulator using thin lithium niobate substrate," in *Proc. OFC/NFOEC*, 2008, pp. 1–3.
[28] Y. Li, L. Zhang, M. Song, B. Zhang, J.-Y. Yang, R. G. Beausoleil, A. E. Willner, and P. D. Dapkus, "Coupled-ring-resonator-based silicon modulator for enhanced performance," *Opt. Exp.*, vol. 16, pp. 13342–13348, 2008.
[29] S. P. Voinigescu, R. Aroca, T. O. Dickson, S. T. Nicolson, T. Chalvatzis, P. Chevalier, P. Garcia, C. Gamier, and B. Sautreuil, "Towards a sub-2.5 V, 100-Gb/s serial transceiver," in *Proc. IEEE Custom Integr. Circuits Conf.*, 2007, pp. 471–478.
[30] M. Chacinski, U. Westergren, B. Stoltz, R. Driad, R. Makon, V. Hurm, and A. Steffan, "100 Gb/s ETDM transmitter module," *IEEE J. Sel. Top. Quantum Electron.*, vol. 16, no. 5, Sep./Oct. 2010, to be published. [Online]: Available: http://ieeexplore.ieee.org/xpl/treeabs_all.jsp?arnumber=5437278.
[31] SHF Communication Technologies, [Online]. Available: http://www.shf.de/
[32] M. Möller, "High-speed electronic circuits for 100 Gb/s transport networks," presented at OFC 2010, San Diego, CA, Paper OThC6.
[33] C. Yu-Chia and L. A. Coldren, "Efficient, high-data-rate, tapered oxide-aperture vertical-cavity surface-emitting lasers," *IEEE J. Sel. Top. Quantum Electron.*, vol. 15, no. 3, pp. 704–715, May/Jun. 2009.
[34] E. K. Lau, A. Lakhani, R. S. Tucker, and M. C. Wu, "Enhanced modulation bandwidth of nanocavity light emitting devices," *Opt. Exp.*, vol. 17, pp. 7790–7799, 2009.
[35] J. Liu, M. Beals, A. Pomerene, S. Bernardis, R. Sun, J. Cheng, L. C. Kimerling, and J. Michel, "Waveguide-integrated, ultralow-energy GeSi electro-absorption modulators," *Nature Photon.*, vol. 2, pp. 433–437, 2008.
[36] S. Bottacchi, A. Beling, A. Matiss, M. L. Nielsen, A. G. Steffan, G. Unterborsch, and A. Umbach, "Advanced photoreceivers for high-speed optical fiber transmission systems," *IEEE J. Sel. Top. Quantum Electron.*, vol. 16, no. 5, pp. 1–14. Sep./Oct. 2010, to be published. [Online]. Available: http://ieeexplore.ieee.org/xpl/freeabs_all.jsp?arnumber=5445020.
[37] J. H. Sinsky, A. Adamiecki, L. Buhl, G. Raybon, P. Winzer, O. Wohlgemuth, M. Duelk, C. R. Doerr, A. Umbach, H. G. Bach, and D. Schmidt, "A 107-Gbit/s optoelectronic receiver utilizing hybrid integration of a photodetector and electronic demultiplexer," *J. Lightw. Technol.*, vol. 26, no. 1, pp. 114–120, Jan. 2008.
[38] A. C. Beling and J. C. Campbell, "InP-based high-speed photodetectors," *J. Lightw. Technol.*, vol. 27, no. 3, pp. 343–355, Feb. 2009.
[39] VI Systems TIA Chips. (2010). [Online]. Available: http://www.v-i-systems.com
[40] C.-F. Liao and S.-I. Liu, "40 Gb/s transimpedance-AGC amplifier and CDR circuit for broadband data receivers in 90 nm CMOS," *IEEE J. Solid-State Circuits*, vol. 43, no. 2, pp. 642–655, Feb. 2008.
[41] Y. M. Suzuki, M. Mamada, and Z. Yamazaki, "Over-100-Gb/s 1:2 demultiplexer based on InP HBT technology," *IEEE J. Solid-State Circuits*, vol. 42, no. 11, pp. 2594–2599, Nov. 2007.
[42] R. E. Makon, R. Driad, R. Losch, J. Rosenzweig, and M. Schlechtweg, "100 Gbit/s fully integrated InP DHBT-based CDR/1:2 DEMUX IC," in *Proc. IEEE Compound Semicond. Integr. Circuits Symp.*, 2008, pp. 1–4.
[43] P. Winzer and R.-J. Essiambre, "Advanced optical modulation formats," in *Optical Fiber Telecommunications V, B: Systems and Networks*, I. Kaminow, T. Li, and A. Willner, Eds. Amsterdam, The Netherlands: Elsevier, 2008.
[44] P. J. Winzer, A. H. Gnauck, G. Raybon, M. Schnecker, and P. J. Pupalaikis, "56-Gbaud PDM-QPSK: Coherent detection and 2500-km transmission," in *Proc. ECOC*, 2009, pp. 1–2.
[45] M. Nakazawa, S. Okamoto, T. Omiya, K. Kasai, and M. Yoshida, "256-QAM (64 Gb/s) coherent optical transmission over 160 km with an optical bandwidth of 5.4 GHz," *IEEE Photon. Tech. Lett.*, vol. 22, no. 3, pp. 185–187, Feb. 2010.

Rodney S. Tucker (S'72–M'75–SM'85–F'90) received the B.E. degree in electrical and the Ph.D. degree from the University of Melbourne, Victoria, Australia, in 1969 and 1975, respectively.

He is currently a Laureate Professor at the University of Melbourne, where he is the Director of the Institute for a Broadband-Enabled Society and the Director of the Centre for Ultra-Broadband Information Networks.

Dr. Tucker is a Fellow of the Australian Academy of Science, a Fellow of the Australian Academy of Technological Sciences and Engineering, and a Fellow of the Optical Society of America. In 1975, he was the recipient of a Harkness Fellowship by the Commonwealth Fund, New York. From 1988 to1990, he was Editor-in-Chief of the IEEE TRANSACTIONS ON MICROWAVE THEORY AND TECHNIQUES. From 1991 to 1993, he was with the Management Committee of the Australian Telecommunications and Electronics Research Board, and a member of the Australasian Council on Quantum Electronics. From 1995 to 1999, he was a member of the Board of Governors of the IEEE Lasers and Electrooptics Society. In 1995, he was the recipient of the Institution of Engineers, Australia, M. A. Sargent Medal for his contributions to Electrical Engineering and was named IEEE Lasers and Electrooptics Society Distinguished Lecturer for the year 1995–1996. In 1997, he was the recipient of the Australia Prize, Australia's premier award for science and technology for his contributions to telecommunications. From 1997 to 2006, he was an Associate Editor of IEEE PHOTONICS TECHNOLOGY LETTERS. He is currently a Vice-President, Publications of the IEEE Photonics Society. In 2007, he was the recipient of the IEEE Lasers and Electrooptics Society Aron Kressel Award for his pioneering contributions to high-speed semiconductor lasers.